A Comparative Analysis of Solar Energy Systems and Photovoltaic Materials

M. Truong[1,4], W. Nguyen[1,4], A. Lostaunau[2,4], L. Holeman[1,4], J. Bryant[3,4], S.A. Curran[4,5]

[1] Department of Biology and Biochemistry, College of Natural Sciences and Mathematics, Science and Research Building 2, 3455 Cullen Blvd #342, University of Houston, Houston 77204, Texas

[2] Department of Psychology, College of Liberal Arts and Social Sciences, 3553 Cullen Blvd, University of Houston, Houston 77204, Texas

[3] Department of Computer Science, College of Natural Sciences and Mathematics, Science and Research Building 2, 3455 Cullen Blvd #342, University of Houston, Houston 77204, Texas

[4] Curran's Nanophysics Research Group, University of Houston, Science & Research Building 1, 3507 Cullen Blvd., Houston, TX 77204 USA

[5] Physics Department, Science and Research Building 1, University of Houston, Houston, 77204, Texas

Abstract

Solar energy conversions rely on diverse systems, including photovoltaic (PV) modules, solar thermal collectors, concentrated photovoltaics (CPV), and concentrated solar power (CSP) towers. The selection and implementation of materials in these systems depend on a balance of materials cost, conversion efficiency, and geographic conditions. Major functional materials range from dominant crystalline silicon to thin film alternatives: amorphous silicon, CIGSe (Copper Indium Gallium Selenide), CdTe (Cadmium telluride). Additionally, materials that aren't thin film include organic photovoltaics, dye-sensitized Grätzel cells, and high-efficiency semiconductors like Gallium arsenide. This review provides a comprehensive analysis of the operational principles, efficiency, and economic factors of these key solar materials and systems.

Introduction

Frank Shuman (1862 - 1918) was an American engineer and inventor who pioneered research into solar thermal energy systems. His contribution laid out the conceptual and practical basis for modern solar systems [1]. His initial success was achieving the commercial patent of his invention of safety glasses; he then transitioned his focus of research to renewable energy due to the concern of rapid depletion and the environmental impacts of fossil fuels [2]. Through his Sunshine Power Company, he spent a decade developing low-pressure steam solar engines, and in 1913 he was able to construct the world's first commercial solar thermal power station in Maadi, Egypt, by using a system of parabolic trough collectors to focus sunlight and power a water pumping engine along the Nile [1,3]. Ultimately, Shuman proved that solar power was no longer theoretical, but could become a practical replacement for traditional fossil fuels [2,3].

Solar energy has become one of the most rapidly deployed and cost-competitive sources of electricity worldwide, driven by dramatic reductions in the levelized cost of electricity (LCOE) and sustained technological progress. In the United States, solar capacity additions reached approximately 43 GWdc (gigawatts direct current) in 2025, with utility-scale projects accounting for the large majority of new installations, followed by residential, commercial, and community systems; solar now supplies nearly 9% of U.S. electricity generation [4]. Resource assessments from the National Renewable Energy Laboratory (NREL) show the highest solar irradiance concentrated in the Southwest, while still supporting viable deployment across the country. The U.S. Department of Energy's Solar Energy Technologies Office (SETO) continues to support research aimed at further cost reductions, targeting roughly $0.03/kWh for unsubsidized utility-scale photovoltaics and $0.05/kWh for concentrating solar-thermal power (CSP) systems with long-duration storage while advancing efficiency, reliability, manufacturing competitiveness, and grid integration [5,6]. Globally, China dominates the production of polysilicon, wafers, cells, and

modules, with leading manufacturers including JinkoSolar, LONGi, Trina Solar, JA Solar, and Tongwei [7]. Along with rapid commercial growth and ongoing research, a wide range of solar cell technologies and system architectures spanning crystalline silicon, thin-film materials (CdTe, CIGSe, amorphous silicon), high-efficiency III–V and multi-junction cells, emerging perovskites and organics, dye-sensitized devices, and both photovoltaic and concentrating solar-thermal configurations continue to evolve [8,9].

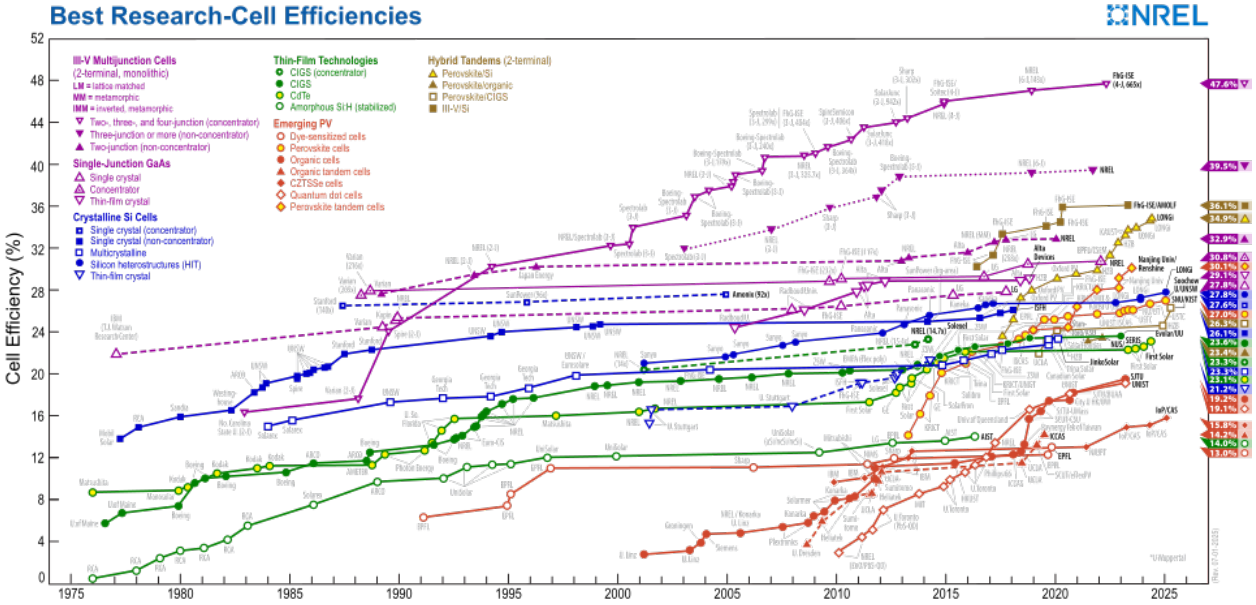


Figure 1. *Conversion efficiencies of best research solar cell worldwide for various photovoltaic technologies since 1976. (Image adapted from Wikimedia Commons, public domain)*

Overview of Concentrated Photovoltaics (CPV) Systems

Solar radiation reaches the upper atmosphere at approximately 166 PW and the Earth's surface at about 85 PW, significantly reducing the sun's full power [10]. Concentrated Photovoltaics (CPV) systems operate by replacing large surface areas of expensive solar cells with systems that concentrate light using lower-cost optical components onto small, highly efficient photovoltaic (PV) cells; overall, this can increase system efficiency while lowering material costs [10]. Current manufacturers' ability to produce these semiconductors is sufficient to meet demand due to the small amount of active PV cells in the systems. Additionally, the surrounding structural and optical

components are readily manufactured worldwide [10]. The reduction in usage of semiconductors in these systems results in a lower usage of toxic materials as well as an increase in more recyclable components, rendering CPV an environmentally friendly alternative to traditional flat-plate PV [10]. Additionally, high-reflectivity mirrors used in CPV systems are susceptible to performance loss from chemical corrosion, photodegradation, physical degradation, and thermal stress [11]; despite these drawbacks, they are still used in certain applications.

Classification of Concentrated Photovoltaics (CPV) Systems

CPV systems are categorized based on the concentration ratio, illumination distribution, focal shape, optical standard, and physical collector design [10]. The primary categorization used is by concentration factor (measured in suns):

Low Concentration Photovoltaics (LCPV): 1 - 40x.

LCPV systems feature lower tracking tolerances, passive heat-sink requirement, lower cost optics, and simplified manufacturing and installation procedures compared to HCPV

Medium Concentration Photovoltaics (MCPV): 40 - 300x

High Concentration Photovoltaics (HCPV): 300 - 2000x

Types of Concentrated Photovoltaics (CPV) Systems

Fresnel Lens Systems

A Fresnel lens is a flat optical component that is made up of many small concentric grooves, with each groove acting as a prism to concentrate light. In early lens applications, polymethylmethacrylate (PMMA) was used, which is an optical material similar to glass. Fresnel systems primarily use optics with Silicon or III-V cells [10]. Some of the major advantages of using Fresnel systems are that they are typically small in volume, lightweight, and easier to mass-produce at low cost [12]. Some major drawbacks are possible light loss due to incident light on the draft

facet, thermal dissipation that requires cooling solutions, and the requirement for sun-tracking systems. There are two major types of Fresnel Lens Systems: Point focus and Linear systems [10].

Point focus systems' typical cost is $1.48/Wp, requires only a passive cooling system and no secondary concentrator, but uses a gimbal tracking system [10].

Linear systems' typical cost is $2.02/Wp, requires a passive cooling system, and requires a secondary concentrator using a solid CPC and a gimbal tracking system [10].

The major applications of Fresnel Lens Systems are through thermal heating, solar cooking, photocatalytic processes, solar building, solar-pumped laser, lighting, and surface modification of metallic materials [10].

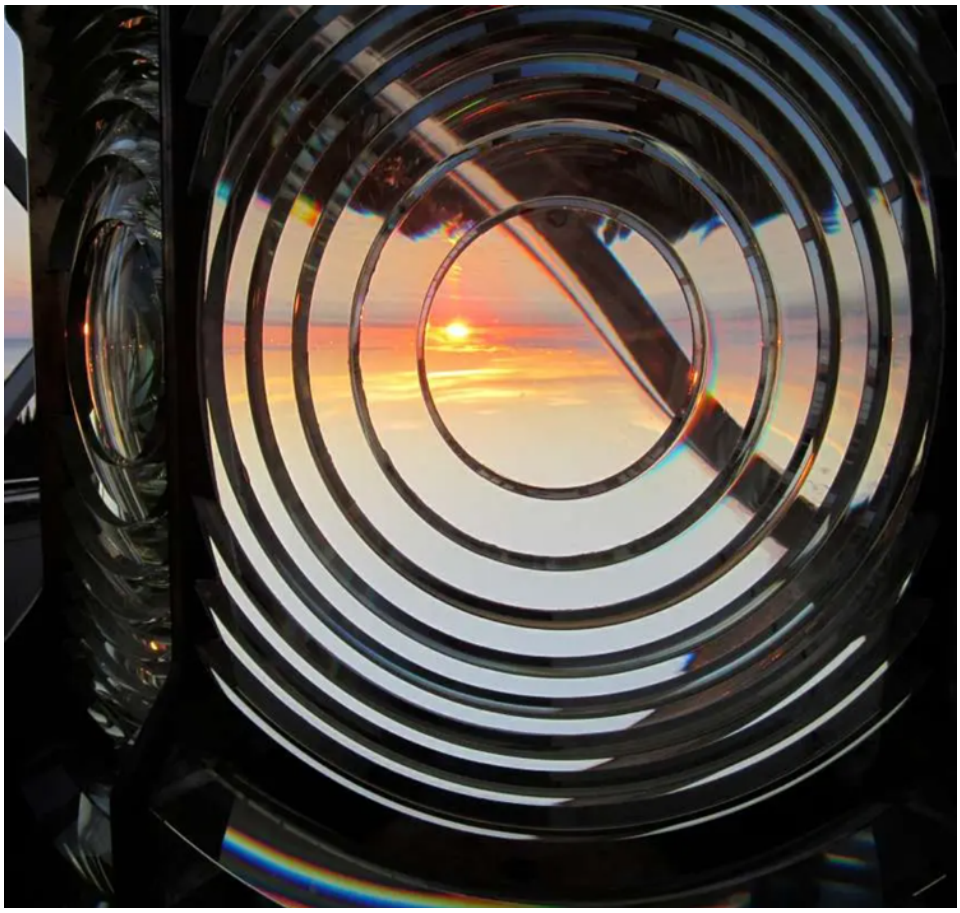


Figure 2. *Fresnel lens (Image adapted from Wikimedia Commons, public domain)*

Quantum Dot Concentrators (QDC)

Quantum Dot Concentrators (QDC) consist of 3 primary parts: a flat sheet of glass or plastic doped with quantum dots, a reflective mirror, and a PV cell [10]. For this system, incident radiation from the sun gets refracted by fluorescent material to be absorbed by quantum dots, which then is able to re-emit photons through total internal reflection toward the PV cell receiver [10]. Main advantages of this system are that the system is nontracking and able to concentrate and diffuse radiation with reduced thermal issues [10] while absorbing light across a large spectrum [13]. The system also comes with its disadvantages that demand strict requirements regarding the use of dyes with high quantum efficiency [10], and that UV exposure and oxidative stress can degrade the QD [14].

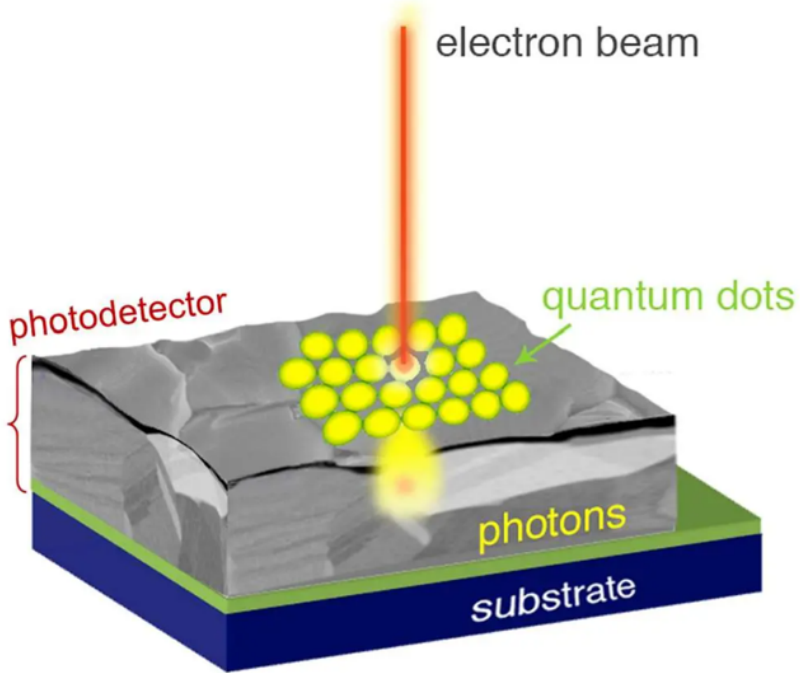


Figure 3. *Quantum Dots (Image adapted from Wikimedia Commons, public domain)*

Parabolic Concentrator Systems

Parabolic concentrators operate by using a parabolic-shaped reflected surface to concentrate and direct solar radiation on a receiver at the focal point [15]. The main cell type used for these applications is Silicon III_V [10]. The advantages of using this system are that they are able to

efficiently utilize direct solar radiation [10] and simultaneously collect thermal energy [15]. In regions with direct sunlight and a lot of available area for these systems, larger-scale models can achieve long-term fuel savings [16]. Generally, cylindrical paraboloid systems that are paired with a point focus secondary concentrator with polar tracking cost $1.78 /Wp [10]. Some drawbacks with these systems are that they are only able to capture direct radiation, leading to requirements for 2-axis tracking, increasing costs [15,16]. Additionally, these systems are sensitive to small imperfections like alignment and surface imperfections, which incur higher costs [10].



Figure 4. *Parabolic Concentrator (Image adapted from Wikimedia Commons, public domain)*

Compound Parabolic Concentrators (CPC)

Compound Parabolic Concentrators (CPC) systems are designed to efficiently collect and concentrate distant light sources in 2D and 3D formats [10]. Additionally, the 3D format is more efficient than 2D systems due to a higher concentration ratio [10]. Some of the advantages of these systems are that no solar tracking is required due to the wide acceptance angle that allows for better capture of light in diffused or scattered forms alongside direct sunlight. Similarly to regular Parabolic Concentrator Systems, one disadvantage is their reliance on direct sunlight. Due to this

reliance, clouds, haze, high humidity, dust, dirt, and pollen can scatter light before it reaches the reflector, which decreases the effectiveness of these systems [17]. Additionally, heating problems come with these systems due to the concentration of light [17]. Despite the higher concentration ratio of these systems, light beyond the maximum half acceptance angle causes temporary drops in efficiency [17].

Dielectric Totally Internally Reflecting Concentrators (DTIRC)

Dielectric Totally Internally Reflecting Concentrators (DTIRC) are a non-imaging optical device that accepts focused solar energy from a primary concentrator and redirects light through refraction and total internal reflection for power generation or propulsion applications. It is primarily designed and studied for spaceflight operations [18]. The benefits of the system are that there is a higher optical efficiency and contraction that CPC's and requires no to minimal cooling systems. Additionally, it features a smaller cavity aperture and a solid crystal structure [18]. Some drawbacks of this system are that it does not efficiently pass all solar energy that it accepts into lower index media, and certain materials used in these systems undergo discoloration and degradation [18]. In applications used in space systems, materials like Zirconia are reduced and turn dark over time when exposed to high temperatures in vacuum, posing operational life limits [18]. Furthermore, in ground testing, MgO degrades in hair due to H2O exposure [18].

Hyperboloid Concentrators

Hyperboloid Concentrators, also known as elliptical hyperboloid concentrators, are one-sheet hyperbolic concentrators that are identified as ideal 3D asymmetric concentrators [10,14]. The major advantages of these systems are that they are very compact [10] and do not disturb the flow lines of an elliptical disk light source, making it ideal as an ideal asymmetric concentration which can be used for non-tracking applications [14]. However, these systems are able to be utilized in

a truncated version that is mainly used as a secondary concentrator [10]. Due to the finite source concentration, it requires an additional asymmetric lens at the entry aperture to convert it into an infinite source concentrator for non-tracking applications [14].

Advanced Refractive/Reflective Architectures (RR, XX, XR, RX, RXI, and Other Custom Optics)

These advanced designs consist of a conventional primary and secondary lens combination using aspheric and total internal reflection components in primary optics to reduce the focal length and module thickness [19].

Mini point focus RXI systems: this system incorporates small lenses, RXI devices, or small parabolic concentrators with silicon or III-V cells at high concentration ratios; additionally, passive cooling and 2-axis tracking are used alongside this system [10].

Curved TIR Lens Systems: A curved TIR lens without a secondary concentrator paired with polar tracking archives a concentration factor of 28 at a cost of $1.97/ Wp [10].

V-trough Systems: A screen-printed V-trough without a secondary concentrator paired with polar tracking achieves a concentration factor of 2 at a cost of $4.31/Wp [10].

Overall advantages of these systems are that it archives the theoretical maximum acceptance angle contraction, high concentration ratios, lighter weights, and less expensive tracking systems [10]. The mirrorless design avoids manufacturability and reliability issues associated with the metallization process from other designs [19]. The general drawbacks of these systems are that the size of the cell needs to be kept to a minimum to reduce the shadowing effect caused by it [10].

Overview of Concentrated Solar Power (CSP) Tower Systems

Concentrated Solar Power (CSP) Tower Systems use mirror/ reflective systems to concentrate solar radiation onto a receiver that is able to convert the concentrated solar energy to high-temperature

heat to generate electricity [20]. The heat is then able to be transferred to a power cycle working fluid to heat water and create high pressure steam that can spin turbines [21]. Solar Power Tower (SPT) systems, also known as central receiver systems, can deliver substantially more energy than standard PV systems [20]. Additionally, in these systems, the solar-to-thermal energy conversion is more efficient than solar-to-electrical conversion in these systems [20]. Despite the benefits of these systems, CSP technologies carry higher initial investment than conventional PV plants but also are able to achieve solar-to-electric conversion efficiency between 20% and 35% [20].



Figure 5. *Aerial view of test facility Sandia National Labs to test Heliostats (Image adapted from Wikimedia Commons, public domain)*

Sections of Concentrated Solar Power Tower Plants

Concentrated Solar Power tower plants are organized into key operational systems: a heliostat collector field, a central tower, a top-mounted receiver, a thermal energy storage (TES) system, a thermodynamic cycle, and a power generation block [20].

Solar Concentration: The collector field is made up of thousands of tracking heliostats, which are mirrors that track the sun to focus solar radiation onto the receiver that top of the central tower [20].

Thermal Conversion: In the receiver, a circulation network of fluid absorbs the concentrated solar energy mainly through thermal energy, heating the fluid to the temperature necessary to produce steam or drive some kind of gas turbine [20].

Power Generation: The high-temperature liquid powers a turbine and a generator to produce energy [20].

Thermal Energy Storage (TES) Dispatch: Excess thermal energy collected during peak irradiance is diverted to a storage system that allows for power to still be used during hours where there is light fluctuation or after sundown [20].

Environmental Factors

Due to Concentrated Solar Power tower plants being largely open to the environment, there are many factors that influence the system's efficiency. Major environmental factors of these systems are the solar irradiance levels, ambient temperatures, local weather, and its effect on daily sun exposure [22]. The efficiency of these systems requires careful planning of their design in how the heliostat field is laid out, receiver configuration, and overall tower height [22]. Aside from the previous factors, there are additional factors that deal with the maintenance of the systems, like heliostat cleaning systems and sun tracking technology to increase their efficiency [22].

Thermal Energy Storage (TES) Media

In TES systems, salts are generally used for these systems and 2 of the common mixtures include [20]. Additionally, solar salts are used in both TES systems and as Heat Transfer Fluid (HTF) in second-generation plants [20]:

HITEC Ternary Salt: 53% KNO_3, 7% $NaNO_3$, and 40% $NaNO_2$ [20].

Binary Solar Salt: 60% $NaNO_3$ and 40% KNO_3 [20].

For third-generation plants, some of the major storage media include:

Advanced Molten Salt Mixtures (MSMs): These are nitrate-based MSMs that are the most commercially mature and affordable [22]. A problem with these salts is that high melting points introduce freezing risks and complex start-up protocols [22]. To combat this, molten salt-based nanofluids are made by dispersing nanoparticles into base salts to increase heat capacity and thermal conductivity [20]. However, this technique can increase fluid viscosity and increase corrosion rates [20].

Phase Change Materials (PCMs): Some common PCMs are $Na_2CO_3+Li_2CO_3$ and $NaF+K_2CO_3$, are able to provide high energy density and compact storage for higher temperatures [22]. However, they suffer from low thermal conductivity and are chemically unstable under heat and have expensive storage requirements [22].

Solid Particle Storage: Materials like white sand, ilmenite, and Carbobead can support temperatures up to 100 degrees Celsius at lower cost [22]. However, material clumping, and system degradation prevent this from being properly utilized [22].

Thermochemical Energy Storage (TCES): Systems like $CaCO_3+CaO$ looping allow for high energy densities and compatibility with closed CO_2 Brayton cycles with theoretical efficiency up to 45% [22]. To prevent CaO sintering during calcination, dopants are able to be added to retain porosity [22]. However, irreversible reaction and complex operational use limits its application [22].

Advantages and Disadvantages

Collector field and heliostats

Major advantages include being highly scalable and capable of concentrating large amounts of solar radiation onto a single point [20]. The major disadvantages of this are that the field is about 50% of the total plant investment and accounts for up to 40% of solar energy losses [20]. Solar tracking systems need constant calibration, and wind-induced deflection and structural deformation can decrease accuracy [22]. To mitigate these factors, additional mechanical sensors and cameras need to be added, which increase the system's complexity and power demand [22].

Receivers

Receivers at the top of towers experience extreme temperatures, fluxes, fatigue, and loss [20,22,23]. Due to this, cavity receivers are selected due to their reduced heat loss compared to cylindrical receivers [23]. Additionally, receiver material directly impacts thermal stress, mechanical integrity, and durability [24].

Stainless steel: Although Stainless steel has high tensile strength, it exhibits the highest thermal stresses and highest stress failure ratio among common alloys [24].

Aluminum: The thermal conductivity of Aluminum is high; it has lower tensile strength compared to other materials [24].

Copper: Copper has the highest thermal conductivity and exhibits the lowest thermal stress and lowest stress failure ratio. Despite this, it has a higher density and greater material cost compared to aluminum [24].

Silicon Carbide (SiC): This material has the highest Young's modulus and a low thermal expansion coefficient, but at higher temperatures it undergoes severe thermal stress and has the second highest stress failure ratio [24].

Global Use of Solar Towers

In recent years, there has been an increase in the use of molten salt media in solar power tower plants [20]. Major investment and project developments expanding beyond 1GW were concentrated across specific regions: United Arab Emirates (UAE), China, Chile, and India during 2020 [20]. Of the CSP systems that have a working net capacity exceeding 150 MW, 4 are currently in the US. These 4 projects are: Genesis Solar Energy Project (Riverside County, California), Mojave Solar Project (San Bernardino County, California), Ivanpah Solar Electric Generating System (San Bernardino County, California), and Solana Generating Station (Gila Bend, Arizona). Genesis Solar Energy and Solana Generating Station have 2 units which when combined is able to achieve a net capacity of higher than 150MW [21], [25], [26]. Currently, Spain holds the number one spot in total installed CSP across all technology types [20]. Despite this, China has the largest number of individual operational or commercial SPT plants installed, and Chile has the largest single share of installed or planned capacity for SPT systems [20].

Photovoltaic Effect and Solar Cells

The photovoltaic (PV) effect describes the process by which charge, or electricity is generated from sunlight [27]. This process involves thin semiconductor materials that provide a pathway for electrons to flow after different materials are struck by sunlight [28]. The absorption of a photon in a p-n junction causes electron-hole pairs to form [29,30]. When the energy in the photon is higher than the gap energy of the semiconductor material in the p-n junction, the electrons are excited, moving from the valence band to the conduction band, leaving these “holes” at the valence level [29].

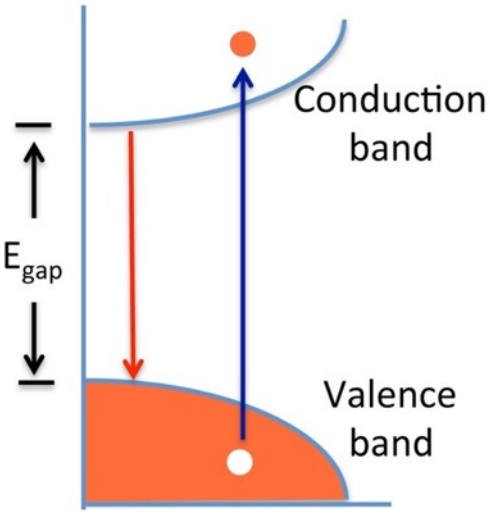


Figure 6. *Electron Hole Pair Leaving Hole in Valance Band (Image adapted from Wikimedia Commons, public domain)*

Solar energy that is absorbed by the semiconductor material causes electrons to be dislodged, creating the mobile electron and mobile electron-hole previously described [30]. The photogeneration of charge carriers occurs when the electron flows to the n-type material while the hole flows to the p-type material [30]. This separation of positive and negative charges creates a potential difference that, when something that takes advantage of the PV effect is connected to a circuit, causes the electrons and holes to travel around the circuit in order to recombine [29,30].

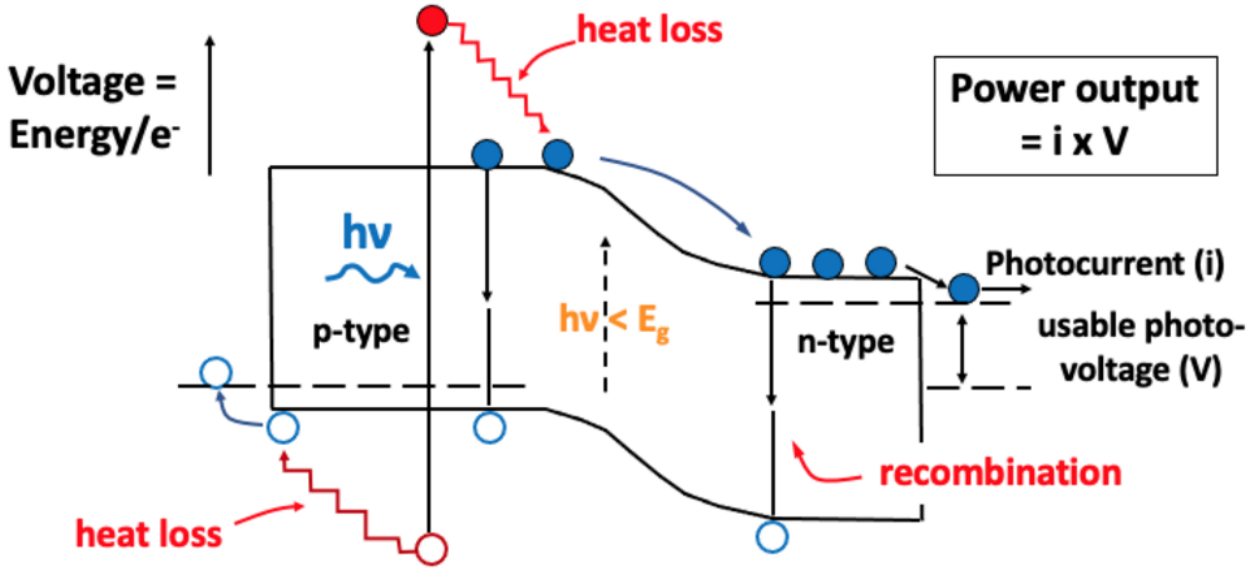


Figure 7. *Current Generation over p-n Junction (Image adapted from Wikimedia Commons, public domain)*

Solar cells are an extremely common use of the PV effect. Solar cells in their most conventional form are, more specifically, silicon solar cells. The cells are made up of a p-n junction that takes advantage of the PV effect. The transfer of electrons and holes across the p-n junction in a solar cell is known as diffusion [29,31], and these charges are generated because the electrons want to recombine with their hole pairs via the equalization of the Fermi energy levels [30,32] in the materials. The electrons want to reach an equilibrium state after their excitation [30].



Figure 8. *Solar Panels (Image adapted from Wikimedia Commons, public domain)*

While photovoltaic cells all take advantage of the PV effect, the materials they use, and the creation of semiconductors vary greatly. PV cells are made from semiconductor materials, typically crystalline silicon (c-Si) [28]. There are two main types of crystalline solar modules: monocrystalline and multicrystalline [27,28]. These crystalline solar modules have been recorded to have the highest efficiencies of all PV devices [30]. However, the process to make them is arduous, requiring a large amount of silicon and a complicated fabrication process to account for the complex composition of c-Si [30]. The common alternatives are using thin film semiconductor materials such as amorphous silicon (a-Si) [28,30]. Due to its thin nature, a-Si is light and flexible,

optimizing itself for a broader range of semiconductor applications. It is also significantly more cost-effective in comparison to the wafer-based technology required for c-Si production [28]. Silicon solar cells can be made using contact formation screen printing. Screen printing is a technique to coat a substrate by rapidly moving a scraper on a patterned metal covered with screen-printing paste [32]. The patterned area of the substrate transfers the paste while the non-patterned area blocks the paste transfer, resulting in the pattern being printed on the film [32]. The semiconductors can then be coated in different materials to increase conductivity or further optimize the semiconductor for PV effect purposes. This is a process that takes advantage of the flexibility of a-Si and is very suitable for thin-film-based systems that would require expensive, complex processes to be converted into semiconductors otherwise. This makes screen-printing with a-Si extremely viable for the p-n junctions needed for solar cells and other PV devices.

These PV cells, or solar cells, are particularly important because of their constant generation of current as long as the cells are absorbing photons. Unlike batteries, PV cells do not need to be charged; as long as they are being struck by sunlight, they are generating usable DC. This makes these PV devices particularly useful for solar energy and renewable energy systems. While PV technology is expanding, the a-Si semiconductors have drawbacks when it comes to efficiency. Single-crystal semiconductors operate at around 20% cell efficiency, while a-Si has a cell efficiency in the 5-7% range [29]. This can be improved by using double- and triple-junction designs, which produce a cell efficiency of around 8-10% [29]. This is still only about half the efficiency that crystal semiconductors can produce. Along with that, thin-film solar cells do see some degradation due to their reaction to the environment. While a-Si semiconductors offer low efficiency and longevity in comparison to c-Si, the cost discrepancy between the two cannot be ignored [29].

Solar Thermal Collectors

Solar Thermal Collectors (STC) are devices that absorb solar radiation and convert it into usable thermal energy [33]. This involves using solar radiation to heat air and water for energy collection purposes. This is achieved in multiple ways with varying purposes. Optimizing optical geometry allows for more potent solar radiation and therefore more intense solar heating [34]. Using different media for transferring the thermal energy provides more efficiency. The solar beams are focused onto some sort of absorbing substrate such as a tube or flat plate, and this heats a transfer of fluid such as synthetic oil or molten salt [34]. The heat transfer fluid then heats some storage media called sensible heat exchangers [34], which can take the form of a liquid or a solid. The primary goal being to store heat by raising the temperature of these media until they can discharge the energy they hold as thermal energy in some system [34,35].



Figure 9. *Evacuated-Tube Collectors (Image adapted from Wikimedia Commons, public domain)*

There are three main types of STC's: flat-plate collectors, evacuated-tube collectors, and concentrating solar collectors [33,35]. Each optimizes a different aspect of the STC process in order to achieve some goal. The flat-plate collectors are widely used for hot water and low-temperature applications since their structure is optimized to reduce visibility as well as being cost-effective

[33]. Evacuated-tube collectors utilize vacuum insulation between the absorber and the material interacting with the solar rays in order to reduce heat loss [33,36]. This makes them particularly effective for environments not optimized for STC's, like places that have less sunlight 104]. Concentrating solar collectors use optical geometry to concentrate sunlight onto a focal receiver to achieve extremely high temperatures that are used for more intense thermal energy operations [33,34]. These methods involve heating some material that interacts with a heat transfer fluid in order to increase the temperature of some heating medium. For evacuated-tube collectors, solar energy hits a glass tube with a copper pipe in it, heating the copper pipe. The air between the copper pipe and the glass pipe is vacuum sealed in order to reduce heat loss [36]. Copper has high conduction properties, which allow it to heat the transfer fluid inside itself, which then transfers the heat to some heat storage unit [36].

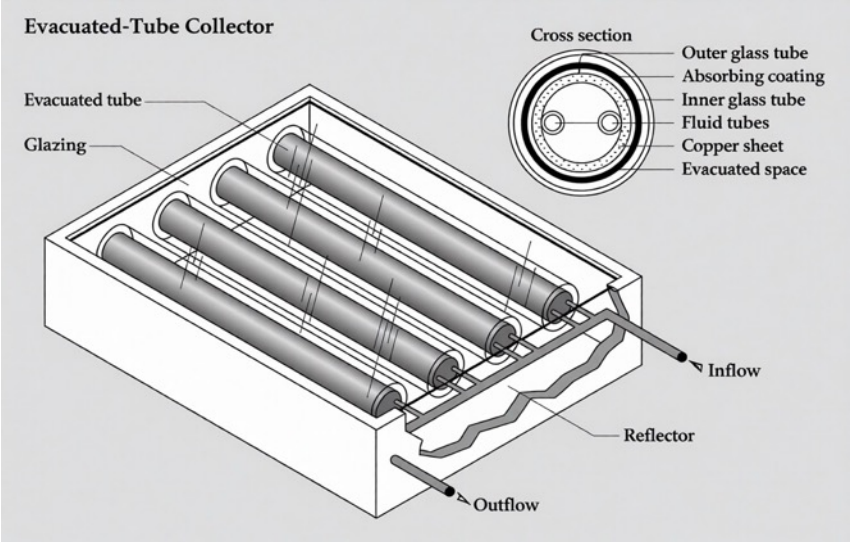


Figure 10. *Inner Makings of Evacuated-Tube Collector (Image adapted from Wikimedia Commons, public domain)*

Flat-plate collectors have around 55% thermal efficiency and an operating temperature of 80 °C – 110 °C (A). Evacuated-tube collectors can reach an efficiency of around 69.5% and temperatures of up to 195.5 °C [33]. These efficiency and temperature metrics are good for most thermal operations; however, for large-scale efficient operations, parabolic collectors that concentrate sunlight, the optical efficiency can reach 92.8% due to the intensity of the beams alone

[33]. Along with this, the other methods for solar collection technologies are relatively cost-effective, achieving a cost of energy ranging from 60 to 100 USD per MWh [34], which is competitive with other conventional energy sources. Maximizing cost in reference to efficiency becomes the sole issue when dealing with environments that already hamper the max efficiency outputs due to weather and lack of sunlight [33,34].

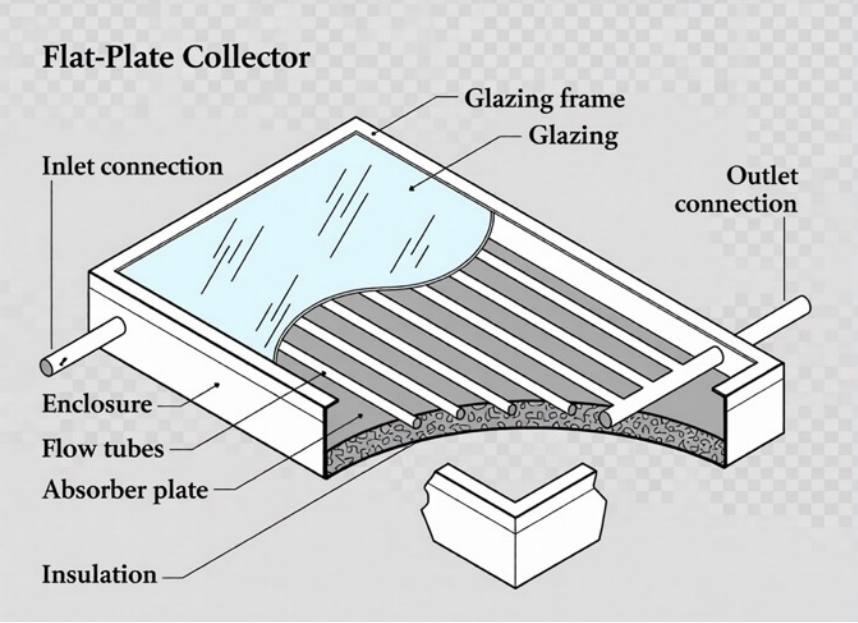


Figure 11. *Inner Makings of Flat-Plate Collector (Image adapted from Wikimedia Commons, public domain)*

Crystalline Silicon

Crystalline silicon solar cells are one of the most well known and highly used types of solar market. This is because of their high energy conversion efficiency compared to other commercially sold solar cells [37]. Silicon possesses an indirect energy band gap, where the valence band maximum and conduction band minimum occur at different points in the momentum space [38,39]. This indirect band gap affects the photovoltaic application of Silicon. Firstly, radiative recombination, the process of an electron in a high-energy state falling down to fill a hole in a lower-energy state, which causes the release of excess energy as a photon, becomes inefficient [40]. Instead, Auger recombination occurs, in which energy released by electron-hole recombination is transferred to a

third carrier and is brought to a higher energy level before it cools down [41]. Also, the indirect band gap results in a low absorption coefficient near the band edge. To combat this, surface texturing and antireflection coatings have been used to enhance the efficiency of light absorption. However, based on these parameters, the theoretical limit of efficiency in solar cells is ~33% [42]. In practical advances, pure elemental silicon is doped with small amounts of boron (p-type) or phosphorous (n-type) to form a p-n junction. Solar-grade silicon begins as quartz that is reduced to metallurgical-grade silicon, which is then purified to reach 99.999% purity. Occasionally, passivation layers, thin, protective outer coating is deposited on the surface of the crystalline silicon solar cells. Typically, silicon nitride, aluminum oxide, or silicon dioxide are used to reduce the recombination of charge carriers on the silicon surface. This technique saturates the bonds by creating a fixed charge that repels carriers away from the interface. This passivation improves the overall cell efficiency, aiding in minimizing optical and electrical losses while also providing antireflection and a moisture barrier [37,43].

Types of Crystalline Silicon

Two main crystalline forms of silicon exist: monocrystalline and polycrystalline (multicrystalline). Monocrystalline silicon cells are made from a single continuous crystal lattice. High material purity causes a nearly perfect lattice which has a weak internal electrical resistance and low grain-boundary energy, excess free energy per unit area [43,44]. The monocrystalline silicon is grown using a single-pulling method, called the Czochralski process, where a single crystal is slowly pulled to produce a uniform lattice [45]. The structural advantages are shown through the higher conversion efficiency. In addition, monocrystalline have a uniform dark color [44]. Polycrystalline, however, is formed from many smaller silicon crystals melted together, their surface shows a dark blue speckled color. The numerous grain boundaries create higher recombination losses and

greater internal resistance, which in turn lowers their efficiency compared to monocrystalline cells [43,44].



Figure 12. *Monocrystalline (Left) and Polycrystalline (Right) Solar Panels (Image adapted from Wikimedia Commons, public domain)*

Efficiency and Cost

Monocrystalline material, specifically, dominate the global solar cell market due to the higher efficiency and lower longterm cost, with roughly 98% of production. The average efficiency of monocrystalline solar cells is 22% - 24%, while polycrystalline efficiency only ranges from 15% - 17% [46]. The higher efficiency from monocrystalline silicon delivers greater power density, meaning more watts per square meter (W/m^2) and thus requiring fewer panels, less roof or land area for the same energy capacity. These cells also show a better temperature coefficient [47] Costs of both monocrystalline silicon modules and polycrystalline silicon modules are varied because of a number of reasons. Monocrystalline modules traditionally have a higher upfront cost because of the Czochralski process used to grow single-crystal ingots is more energy-intensive and produces some silicon waste, while polycrystalline modules benefit from a simpler casting method that historically kept their price lower [48]. In recent years, the cost gap has narrowed, due to more efficient manufacturing monocrystalline panels costing between $0.70 to $1.50 per watt, while polycrystalline panels cost $0.60 to $1.20 per watt [49]. Although monocrystalline panels may still cost slightly more to purchase, their higher efficiency, greater power density, and superior lifetime energy yield frequently result in a lower levelized cost of electricity and better long-term return,

especially where space is limited, or high irradiance is available. Polycrystalline modules retain a modest cost advantage in some budget or large ground-mounted projects where land is inexpensive, but their lower efficiency means more modules are needed to reach the same capacity, which can offset the initial savings [46].

Application

Real-world outdoor monitoring reveals that climate strongly influences the relative efficiencies of both crystalline solar cells. In a semi-arid environment with high solar irradiance, the instantaneous power from the Sun received per unit area of Earth's surface, monocrystalline modules delivered higher maximum efficiency and a greater overall energy yield across a full year, even though their energy efficiency noticeably declined during the hottest months [50,51]. A multi-year study in a temperate semi-arid climate, similarly, found that south-facing monocrystalline systems achieved the highest efficiency and performance ratio among several other configurations. A monocrystalline Passivated Emitter and Rear Cell (PERC) module, which has an extra coating that reflects unused light back through the silicon to generate extra power, was placed under partial shading and proved to be more resistant to hot spot formation [43,52]. In the study, it showed that a single cell needed approximately 60% shading to reach a dangerous temperature near 90°C whereas polycrystalline PERC modules developed hotspots at only 40% shading and suffered greater power and efficiency losses [43].

In contrast, an arid-region study focused on high temperatures and dust showed that polycrystalline modules experienced smaller relative power drops (14% versus 16%) under high irradiation as temperatures rose. Under low irradiation the reverse was true; monocrystalline modules only lost about 9% of power compared with 21% for polycrystalline [53]. Dust effects also varied with light level; monocrystalline modules were more affected under strong sunlight, while polycrystalline modules suffered more under weak light [53,54].



Figure 13. *Field of monocrystalline solar panels (Image adapted from Wikimedia Commons, public domain)*

Overall, studies indicate that monocrystalline modules are generally superior in efficiency, energy yield, space utilization, aesthetics, and resistance to shading-induced hot spots. They perform especially well in moderate-to-high irradiance conditions when optimally oriented. Polycrystalline modules can be more temperature-tolerant under intense heat and high irradiance and may retain a cost or stability edge in certain arid environments [48,52,53,54,55]. The optimal choice therefore depends on local climate (temperature, irradiance intensity, and dust), orientation, and whether the priority is maximum efficiency, specific yield, or long-term thermal resilience.

Amorphous Silicon

Amorphous silicon (a-Si) is a non-crystalline, hydrogenated form of silicon in which the atoms lack long-range order. Unlike crystalline silicon, the atomic network is disordered, creating a high density of dangling bonds that act as deep electronic traps and recombination centers. Hydrogen

atoms passivate these bonds that improve the electronic quality of the material [56]. Without sufficient hydrogen, pure amorphous silicon is not viable as a semiconductor for solar cells [56,57].

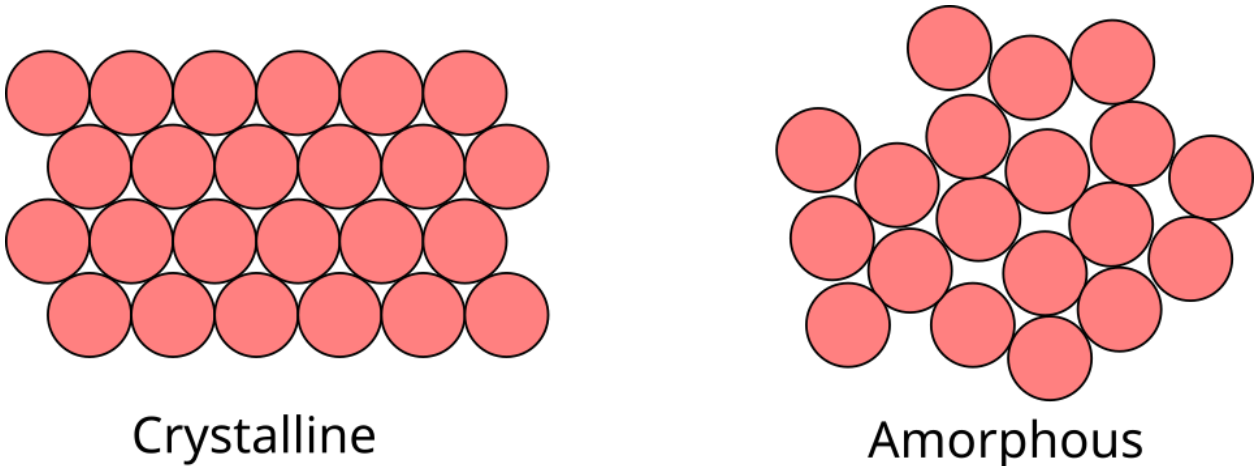


Figure 14. *Structure of crystalline and amorphous solids. (Image adapted from Wikimedia Commons, public domain)*

Manufacturing

In amorphous silicon solar cells, the device is built as a p-i-n structure rather than a simple p-n junction. Three layers are deposited sequentially using plasma-enhanced chemical vapor deposition (PECVD) [58]. Firstly, a thin p-type layer that is boron-doped is deposited. A thicker undoped intrinsic layer of hydrogenated amorphous silicon that acts as the main light absorber is then deposited; and finally, a thin n-type layer that is phosphorus doped.

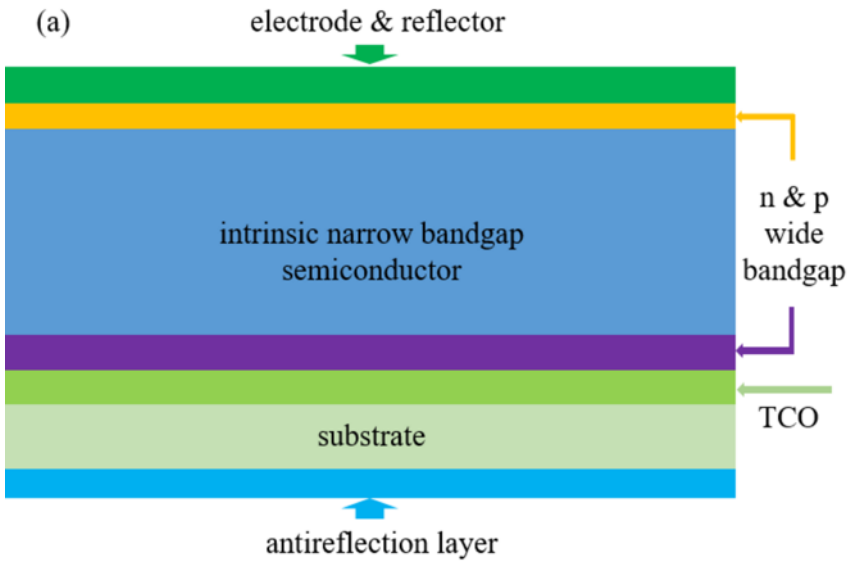


Figure 15. *P-i-n layered diagram of an amorphous silicon solar cell (Image adapted from Wikimedia Commons, public domain)*

These doped layers establish a strong built-in electric field along the intrinsic region [58,59]. When sunlight is absorbed in the intrinsic layer, electron-hole pairs are generated. Because amorphous silicon has very short carrier diffusion lengths, because of the random atomic network, a p-n junction would collect almost no current [60]. The thickness of the doped layers is kept ultrathin, ranging from 10-30 nanometers, so they absorb as little light as possible, while the intrinsic layer is several hundred nanometers thick to absorb sufficient sunlight [57,60]. The same structure can be deposited in reverse order as an n-i-p stack when the substrate or process sequence requires it. This p-i-n structure forms the foundation of both single-junction and multi-junction amorphous silicon solar cells [56,58,59,61].

The optical absorption coefficient of amorphous silicon is around 40 times higher than that of crystalline silicon across much of the visible range, so only a very thin layer is needed to absorb most incident light. The optical (Tauc) bandgap is wider, approximately 1.7 eV versus 1.1 eV for crystalline silicon [56]. This shifts the absorption edge toward the blue–green portion of the spectrum and gives a-Si cells an advantage under diffuse light, indoor lighting, and certain cloudy conditions [58].

Single-junction amorphous silicon solar cells use one light-absorbing layer within a p-i-n structure. These cells are generally inexpensive and straightforward to manufacture, as they only require a sequential PECVD process, consume very little material, and can be deposited on low-cost or flexible substrates such as glass, stainless steel, or plastic [57,59]. The main drawback is light-induced degradation caused by the Staebler-Wronski effect. This effect states that prolonged illumination creates bond defects in the amorphous network, increasing recombination and reducing efficiency. As a result, single-junction cells commonly lose 20 - 30% of their initial efficiency through hours of light exposure [62]. Thicker absorbers needed for higher current suffer even greater losses because carrier collection becomes less efficient once defects form. Stabilized laboratory efficiencies typically reach only about 9–10 percent, while commercial modules are often lower [60].

Multi-junction amorphous silicon cells address the limitations of single junction cells by stacking two or three p-i-n junctions in a series, each specified for different band gaps [56,63]. The top cells use a wider bandgap intrinsic layer, so that it absorbs the higher energy blue and green photons while allowing lower-energy light to pass through. The middle and bottom cells use a narrower bandgap intrinsic layer such as amorphous silicon-germanium or microcrystalline silicon that absorbs the remaining red and near-infrared light. This approach allows the overall device to utilize a broader portion of the solar spectrum while reducing thermalization losses [57,58]. Individual layers can remain thinner than in a comparable single-junction cell, which lessens the impact of the Staebler–Wronski effect; thinner absorbers mean fewer recombination losses even after defects form. As a result, multi-junction devices typically show only half the relative efficiency drop of single-junction cells under the same light-soaking conditions and achieve higher stabilized efficiencies, historically reaching the low-to-mid teens percent in laboratory devices [61,64]. Commercial device efficiencies typically fall between 6% and 12%. Laboratory single-junction cells

have reached about 10.2 %, while optimized multi-junction devices have demonstrated stabilized efficiencies in the 13–14 % range [62].

Application

Temperature coefficients for stabilized amorphous-silicon modules are more favorable than those of crystalline silicon, typically –0.20 to –0.30 %/°C for power versus roughly –0.35 to –0.45 %/°C for crystalline silicon [65]. In hot climates or during summer months, elevated module temperatures enhance thermal annealing and partially recover efficiency lost to the Staebler–Wronski effect, so modules often perform best in warm weather. In cooler climates or winter, annealing slows while light-induced degradation continues, causing efficiency to dip. The amorphous-silicon response is stronger in the blue–green region, making the redder winter spectrum less favorable and the summer spectrum better matched. Low-light performance remains strong because of the high absorption coefficient, allowing amorphous-silicon modules to outperform crystalline silicon under heavy overcast or indoor conditions relative to their standard-test ratings [65,66,67,68]. Humidity and moisture pose greater long-term reliability risks as inadequate sealing can lead to corrosion or degradation under damp and hot conditions. In hot-humid tropical environments the beneficial annealing from high temperature must be balanced against the reliability risks of high humidity [66,69].

Cost

Historically amorphous silicon was attractive because it uses only a small fraction of the silicon required for wafer-based cells and because PECVD is a relatively low-temperature, large-area process compatible with continuous manufacturing [57,70]. Therefore, the material cost per watt was low. In the late 2000s and early 2010s, when crystalline silicon prices were high, thin film silicon became a large part of the solar cell market. Soon after, crystalline silicon manufacturing

scaled dramatically which allowed them to be produced and sold much cheaper and in larger quantities than amorphous silicon [59,71]. Pure a-Si modules became a niche product. Small off-grid panels are still available and cost between $0.70 to $1.00 per watt. Energy return time remains favorable due to the low process temperatures and very small amount of material required [72]. However, the lower conversion efficiency demands a larger area to produce the same power. For this reason, a-Si is rarely competitive in ground-mounted or standard rooftop installations today. Its commercial niche is limited to uses in which form factor, weight, flexibility, low-light response, or visual integration outweigh pure efficiency and cost per watt: small consumer devices, thin-film transistors for LCD screens, and x-ray imagers [72,73,74].



Figure 16. *Amorphous solar cell used in handheld calculators (Image adapted from Wikimedia Commons, public domain)*

In summary, studies indicate that amorphous silicon lag behind crystalline silicon in efficiency, energy yield, and space utilization, yet they offer advantages in low-light performance, temperature coefficient, flexibility, and very low material use. They perform relatively well in diffuse or low-irradiance conditions and in applications where weight, form factor, or aesthetic integration matter more than peak power density. The optimal choice therefore depends on whether the priority is absolute efficiency and cost per watt or low-light response, mechanical flexibility, and form-factor constraints.

Organic Photovoltaics

Organic photovoltaics use carbon-based conjugated molecules as the light-absorbing and charge-transporting materials. Unlike inorganic semiconductors, organic materials generate tightly bound excitons upon photon absorption [75]. These excitons diffuse to a donor–acceptor interface where they dissociate into free charges driven by the energy-level offset between the two materials. Structure control is critical for efficient charge generation and transport. Radiative recombination is possible but usually inefficient; the dominant losses are non-radiative recombination and incomplete exciton diffusion to an interface [76,77].

Manufacturing

Single-junction OPV devices are typically fabricated by solution processing rather than high-temperature crystal growth. It relies on a bulk heterojunction (BHJ) rather than a doped p-n junction because organic semiconductors have low dielectric constants, light absorption creates tightly bound excitons instead of free charges [78,79]. These excitons need a nearby donor–acceptor interface to split, so a bulk heterojunction provides the large interfacial area required for efficient charge generation. A transparent conductive electrode (indium tin oxide on glass or flexible plastic) is first coated with a thin hole-transport layer such as poly(3,4-ethylenedioxythiophene) (PEDOT: PSS) [78]. The photoactive bulk-heterojunction layer is then deposited from a blended solution of a conjugated polymer or small-molecule donor and a non-fullerene acceptor in an organic solvent, most often by spin-coating or by scalable methods such as slot-die coating, blade coating, or roll-to-roll printing for larger areas [75]. After solvent evaporation and optional thermal or solvent-vapor annealing to optimize phase separation, an electron-transport layer and a reflective metal cathode are added. The entire stack is finally encapsulated to protect the organic materials from oxygen, UV exposure, and moisture. This low-

temperature, solution-based route enables thin, lightweight, and potentially flexible modules at relatively low material consumption [76,77,78].

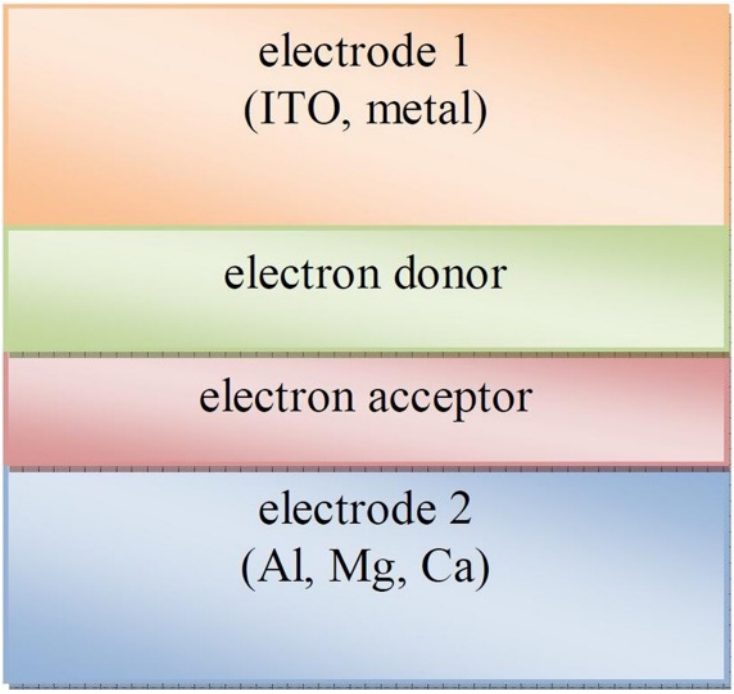


Figure 17. *Multilayer organic photovoltaic cell (Image adapted from Wikimedia Commons, public domain)*

Efficiency

Laboratory single-junction organic photovoltaic cells have advanced rapidly, with power conversion efficiencies now reaching 19–20% in optimized polymer/non-fullerene acceptor systems, a substantial rise from the single-digit values typical of early fullerene-based devices [79]. This progress stems mainly from improved light absorption into the near-infrared, reduced voltage losses, and better control of bulk-heterojunction morphology. Theoretical limits remain lower than the ~33% Shockley–Queisser ceiling, the highest level of efficiency for a single layer solar cell, of ideal inorganic cells because of the energetic cost of exciton dissociation and higher non-radiative recombination rates; realistic single-junction targets under standard sunlight are placed in the mid-20% range [80,81]. Commercial OPV modules currently deliver lower efficiencies, often in the high single digits to low teens, illustrating the challenges of scaling area, maintaining morphology, and ensuring long-term stability. Even so, the combination of rising laboratory performance,

solution processability, and unique form-factor advantages continues to narrow the practical gap with established technologies for selected applications [82,83].

Organic photovoltaic materials typically exhibit high absorption coefficients, often exceeding 10^5 cm^{-1}, which allows efficient light harvesting in active layers only 100–300 nm thick [84,85]. Early polymer donors such as poly(3-hexylthiophene-2,5-diyl) (P3HT) absorbed mainly in the visible range, limiting the electric current that flows through the cell, but modern non-fullerene acceptors (especially the Y-series) have strong absorption into the near-infrared, enabling coverage of a broader portion of the solar spectrum when paired with wide or medium bandgap donors. The combination of strong, adjustable absorption and nanoscale mixing strengthens the high short-circuit currents now achieved in single-junction OPV devices [79,82].

Applications

Real world application studies show that climate strongly modulates relative performance. In hot, high-irradiance environments, some OPV modules exhibit a positive temperature coefficient (efficiency rising with temperature). This can partially offset thermal losses. Performance under low-light or diffuse conditions is often superior because of the high absorption coefficients and favorable spectral response of modern non-fullerene systems. Dust reduces current output, and humidity/condensation can accelerate degradation if encapsulation is imperfect. Long-term outdoor tests (multi-year deployments in tropical, temperate, and arid climates) report degradation rates that vary widely with architecture and packaging; well-encapsulated non-fullerene devices have retained >80–90% of initial performance after many months under real-world conditions, though initial degradation and gradual morphological or chemical changes remain challenges. Partial shading behavior depends on cell interconnection and series resistance; hotspot formation is generally less severe than in silicon because of lower current densities, but thermal and photochemical stress still occur [86,87,88,89,90].

Cost

Organic photovoltaics offer the potential for low manufacturing costs because they rely on solution processing at relatively low temperatures and consume very little active material [76]. Roll-to-roll printing on flexible plastic substrates can further reduce capital and energy costs compared with the high-temperature crystal growth and wafering required for crystalline silicon. In practice, however, current commercial OPV modules remain more expensive on a dollars-per-watt basis than mainstream silicon panels, typically ranging from roughly $0.50 to $2.00 per watt and sometimes higher for small-area or specialty modules [82,91]. The higher cost stems from expensive specialty chemicals, especially high-performance non-fullerene acceptors, transparent electrodes, high-barrier encapsulation needed for lifetime, and still-limited production scale [91]. As material synthesis is simplified, encapsulation improves, and manufacturing volumes increase, the cost gap is expected to narrow, particularly for applications that value flexibility, light weight, or semi-transparency rather than pure power.

Overall, organic photovoltaics have advanced from early low-efficiency devices to laboratory single-junction cells approaching 20%, thanks to improved materials, bulk-heterojunction morphology control, and broader spectral absorption. They remain less efficient and currently more expensive per watt than crystalline silicon, and they still face challenges of early performance loss and long-term outdoor durability. Yet their unique combination of flexibility, light weight, semi-transparency, and low-temperature solution processing makes them well suited to applications where conventional rigid panels are impractical; building-integrated systems, portable power, indoor sensors, and agrivoltaics.

Copper Indium Gallium Selenide

Copper Indium Gallium Selenide (CIGSe) solar cells have increased in popularity within the photovoltaic market due to its tunable band gap and capability to enhance absorption efficiency without affecting its thin layer [92]. CIGSe has a direct bandgap, in which the top of the valence band occurs at the same value of momentum as the bottom of the conduction band. This prevents the need for extra momentum for electrons to absorb light energy [93]. However, CIGSe is capable of having the band gap adjusted from 1.0 eV to 1.7 eV by altering the ratio between Gallium and Indium. By increasing the amount of Gallium compared to the amount of Indium present in the solar cell, the valence band will begin splitting and have a larger energy difference between the conduction band. As the energy difference begins to increase, CIGSe is able to absorb lower-energy photons within the band gap range [92,94,95]. When combined with other materials with large bandgaps, both materials are able to match band gap widths to increase overall efficiency [92,94,95].

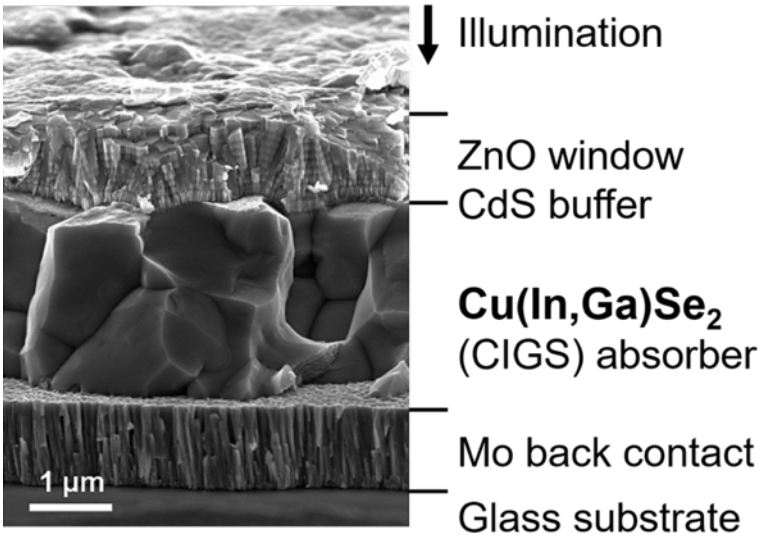


Figure 18. *Cross-section of a CIGSe solar cell showcasing the different layer composition (Image adapted from Wikimedia Commons, public domain)*

CIGSe solar cells have a unique, yet complex structure due to materials being stacked over one another, leading to potential reactions within the layers [96]. Substrate configuration is the

most common configuration, with soda-lime glass acting as the bottom of the cell allowing for light to enter through the top layer [96,97,98]. Choosing an appropriate substrate is crucial as it can directly affect the properties of any materials deposited onto the surface. Molybdenum acts as the back contact due to its stability at high temperatures and having a low contact resistance when in contact with the p-type absorber layer, CIGSe, which is deposited on top [94,96,99]. Having multiple absorber layers can combat the necessity to consistently tune the band gap of one absorber layer. With a higher concentration of Gallium on top, a lower concentration on the bottom, and CIGSe in the middle, both open circuit voltage and short-circuit current density can be improved for increased solar efficiency [100]. However, introducing multiple absorber layers to increase the band gap may result in complications with the buffer layer. Cadmium Sulfide (CdS) is an n-type semiconductor that is most commonly used as a buffer layer with CIGSe solar cells. This is due to CdS having a higher band gap of 2.4 eV, compared to CIGSe without any tuning at 1.1 eV, allowing for more photons to reach both the junction and absorber layer [96,100]. As the band gap of CIGSe increases due to adding multiple absorber layers, a conduction band offset occurs that results in a decrease of electron-hole pairs. These electron-hole pairs are crucial in converting sunlight into electrical power [96,100,101]. Studies have begun looking for alternatives to CdS due to its toxic nature, such as zinc-based compounds [94,100,102]. Zinc oxide (ZnO) can be utilized as an n-type buffer substitute due to its capabilities of transmitting photons in the blue spectrum by having a higher band gap than CdS of 3.37 eV [96,100]. Aluminum-doped ZnO rests on top of the buffer layer and is commonly used as both a transparent conducting oxide (TCO) and front contact, with conductivity being dependent on the mobility and carrier concentration that can also be enhanced through crystallization [95,96].

There has been increased attention for CIGSe solar cells within the market due to its efficiency consistently being above 20% and its capabilities surpassing other solar cell materials

[103]. CIGSe photovoltaic panels offer more flexibility compared to silicon and cadmium telluride (CdTe), along with maintaining a thin film structure with a wide absorption range [39,40,103]. However, material availability and production costs have significantly impacted its usage. Indium is considered an endangered element as almost 90% of its supply is obtained as a byproduct of zinc mining [103,104]. Indium production is concentrated in Peru and Canada, with China leading the industry of indium production at 43-66% control over indium reserves across the globe [37,104]. A typical CIGSe solar cell utilizes 10-15% indium, which will increase the overall cost of raw materials. Due to the scarcity of indium, CIGSe sells at roughly $0.60 per Watt, which is more costly than cadmium telluride (CdTe) and gallium arsenide (GaAs), but cheaper than amorphous silicon [105,106]. Recovering these materials has been a challenge due to the number of materials within a solar cell at such a low concentration. Methods have been proposed in recycling these materials through high temperature, leaching, and separation and purification steps. However, a lot of energy and chemicals are utilized in order to separate these materials [41].

While solar cell efficiencies are determined to be most optimal within laboratory settings, outdoor conditions are real indicators on a materials' overall performance. Arid regions with little to no moisture have shown to enhance CIGSe efficiency due to its ability to handle high temperatures [107,108,109]. CIGSe has a smaller temperature coefficient and by increasing the temperature, photons have enough energy to overcome the reduction in band gap energy to increase the current of photons generated [107,108,109,110]. However, once moisture is introduced into the air, the materials within the solar cell begin to degrade and result in an increase of contact resistance of the TCO. This leads to an overall decrease in performance and efficiency due to the trapped moisture that seeps in through the front contact [107,109,110,111]. When it comes to the amount of sunlight present, CIGSe are capable of performing well in both sunny and cloudy conditions. While there is a significant increase in performance when CIGSe is susceptible

to straight sunlight, the structural stability and broader absorption spectrum allows for the cell to remain optimal in cloudy conditions [109].

CIGSe are highly efficient thin-film solar cells that have proven to have an overall efficiency that continues to increase over time. From optimal performances in dry weather conditions to capabilities of adjusting the band gaps for peak efficiency, CIGSe is an excellent substitute for thin-film solar cells. However, operational costs and scarcity of materials needed to manufacture these cells has prevented its usage in many regions across the globe.

Cadmium Telluride

Cadmium Telluride (CdTe) have become more attractive to the photovoltaic market due to their increased efficiency and low production costs. Compared to silicon solar cells, CdTe has led the market in commercial success for being the most cost-effective and ability to be easily manufactured [112,113]. CdTe is a p-type semiconductor with a direct band gap of 1.45 eV, matching the solar energy emission maximum of 1.5 eV. This allows for CdTe to absorb 99% of photons that have energies larger than the band gap [112,113,114]. While the band gap range is susceptible to adjustments, another material such as zinc or selenium would need to be added to achieve a wider range. With these materials, the band gap has potential to decrease in eV rather than increase, whereas compared to CIGSe solar cells, the band gap is tunable based on adjusting the ratio of materials within its composition [115].

CdTe solar cells have a similar configuration to CIGSe solar cells, but rather in the opposite order. Superstrate configuration is the inverse of substrate configuration, where the substrate is hit with light first then being absorbed by the solar cell [116]. For this configuration to be successful, the substrate needs to be transparent and able to react well with the transparent conducting oxide (TCO) layer that will act as the front contact. Glass is the most commonly used

substrate due to its stability and protection against environmental influences; however, glass is susceptible to cracking and has a rigid structure, preventing much flexibility with the solar cell [113,116]. Zinc-based compounds such as zinc oxide (ZnO) are primarily used as the window layer that rests on top of the TCO layer based on having a greater surface area [117]. CdTe is used as the p-type absorber layer that pairs well with cadmium sulfide (CdS) as the n-type buffer layer to form a heterojunction. This heterojunction allows for electron-hole pairs to form and conduct a current, along with producing a magnetic field just above the depletion zone where the holes formed [117,118]. However, cadmium is relatively toxic and with an increased amount of cadmium in both the absorber and buffer layers, can result in potential health complications [117,119]. The back contact is deposited over the buffer layer that can maintain long-term stability of the solar cell. Copper has notedly been used as the back contact, however, studies have shown that copper diffuses through the grain boundaries of the cell and goes across the junction. This results in recombination to occur as copper will catch electron carriers and leave them ineffective, degrading its efficiency [113,120]. Due to these complications, zinc or aluminum-based compounds are more appealing as back contacts to avoid rapid diffusion of ions across the solar cell [120,121].

While CdTe has an efficiency of roughly 18-19%, the structural integrity of these solar cells prevents efficiency from reaching all-time highs. CdTe has a polycrystalline structure that is made from multiple grains, ranging from 0.7 to 0.1μm. These grain boundaries can result in deep gap states, which are energy levels that are deep within both the valence and conduction bands that capture free charge carriers. These gap states can allow for recombination to occur and significantly decrease overall performance of CdTe solar cells [122,123,124]. To combat this issue, cadmium dichloride ($CdCl_2$) can treat CdTe films to enhance current flow across the grain boundaries. $CdCl_2$ acts as an annealing aid by immersing CdTe in a solution with $CdCl_2$ at very

high temperatures. However, residue may be left on the film that begins to react with the TCO. Studies have shown that a physical vapor deposition process is also a viable alternative to annealing but is more costly compared to simply annealing [123,124].

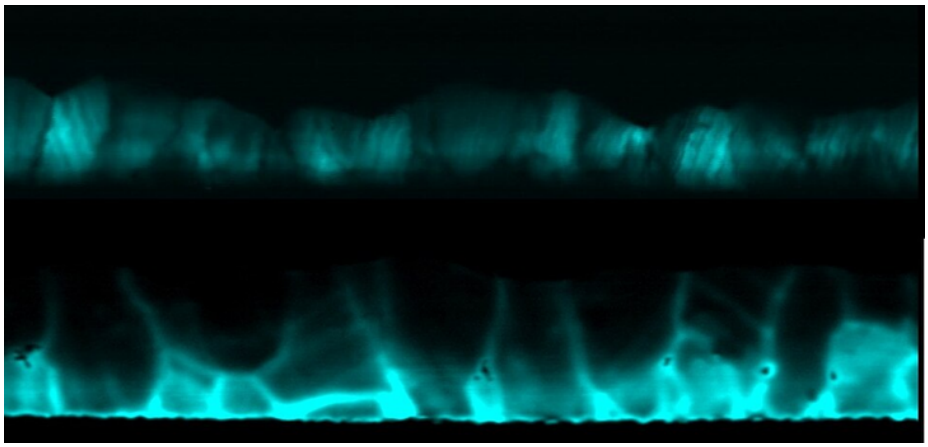


Figure 19. *Grain boundaries in CdTe solar cells. Top shows grain boundaries before treatment, bottom shows grain boundaries after treatment with* $CdCl_2$ *(Image adapted from Wikimedia Commons, public domain)*

First Solar is an American publicly traded manufacturer of solar panels based in Arizona where they specialize in manufacturing CdTe solar panels [125]. Arizona is known for its hot, arid climate in which solar panels need to be designed to withstand high temperatures and perform at optimal efficiency. In a one-year study determining performances of CdTe solar cells in hot, arid climates, efficiency continued to increase as temperature began climbing [126]. This is due to CdTe having a lower temperature coefficient, allowing for less energy to be lost when temperature begins to rise. Compared to other manufacturing companies, First Solar is capable of manufacturing these solar panels within one facility, compared to other companies that have multiple facilities to process raw materials, allowing for cheaper manufacturing costs [125]. With CdTe solar cells being produced for as little as $0.46 per Watt and efficiency being nearly 19%, these solar cells are more cost-friendly compared to crystalline panels and capable of having a high performance in both hot, sunny climate and low-light environments [127].

Gallium Arsenide

Gallium Arsenide is a chemically bonded compound semiconductor consisting of gallium (Ga) and arsenic (As) that is utilized in a variety of optoelectronic and photovoltaic devices due to its direct band gap, high electron mobility, electron saturation velocity, optical properties, and radiation resistance. Direct band gaps allow electrons to move between the valence and conduction bands without requiring a change in momentum and induce a high probability of photon absorption near the band-gap energy [104]. High electron mobility results in rapid electron movement with little resistance or scattering to encourage high operation speeds optimal for high-speed electronics, while high electron saturation velocity causes negative differential resistance (NDR), a decrease in average electron velocity under an applied electric field. At sufficiently high electric fields, electrons within the conduction band can transfer from low-energy valleys to high-energy valleys and the resulting NDR is used in instruments such as the Gunn device to generate microwave oscillations through reinforced electrical fluctuations [128].

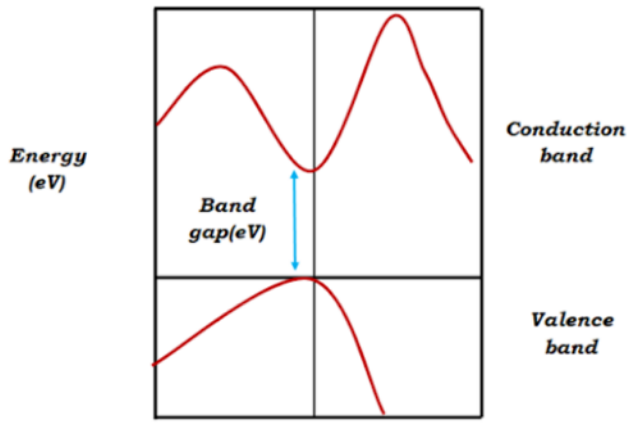


Figure 20. *Modified band gap diagram of gallium arsenide (GaAs), adapted from [129], licensed under CC BY-SA 4.0.*

Optical properties such as gallium arsenide's reflectivity and refractive index change with photon energy, so the compound doesn't reflect the same percentage of radiation across the entire electromagnetic spectrum. In lasers and LEDs, controlling semiconductor surface reflection regulates the transmission and emission of light from the device and its small dielectric constant

facilitates the quick propagation of electric signals through device structures. Irradiation-induced defects are a major challenge for space-based photovoltaic devices, but GaAs solar cell high-energy charge carriers reduce their effectiveness to create an overall radiation resistance for the material.

High-quality GaAs crystals are grown using several epitaxial techniques such as liquid-phase epitaxy (LPE), metal-organic vapor-phase epitaxy (MOVPE), and molecular beam epitaxy (MBE). LPE utilizes GaAs crystallization out of a supersaturated liquid solution to impart a thick, epitaxial semiconductor layer onto a crystalline substrate under thermodynamic equilibrium conditions, while MOVPE reacts gaseous metal-organic precursors at the heated substrate surface to form a thin, multi-layered epitaxial layer. MBE, on the other hand, directs molecular or atomic beams onto a heated substrate under high vacuum conditions to precisely control the film thickness on the atomic and molecular interfaces of the GaAs crystals [128,130]. High-quality crystals minimize structural defects while improving carrier lifetimes to preserve the electronic properties required for optoelectronic applications.

Manufacturing bulk GaAs crystals proves challenging because gallium has a stronger affinity for oxygen than arsenic, so its oxidation under high temperatures leaves most bulk GaAs crystal samples arsenic-rich. Additionally, the high vapor pressure of arsenic makes it more volatile than gallium at high temperatures, and its evaporation leaves many bulk GaAs crystal samples gallium-rich. Imperfections in the Ga:As stoichiometric ratio introduce additional energy levels within the band gap that obstruct charge carrier activity and decrease electrical activity. In response to these issues, the liquid encapsulation technique layers molten boron oxide over the Ga:As melt to reduce arsenic loss and protect the melt from the surrounding atmosphere. While this technique maintains the Ga:As stoichiometry required for producing high-quality bulk GaAs crystals, interactions between the encapsulant and the melt introduce additional contamination, defect, and quality issues [128].

Grätzel Cells

Grätzel Cells, also known as dye-sensitized solar cells (DSSC), are photovoltaic devices that use a thin, porous film of titanium dioxide nanoparticles coated with a light-absorbing dye to convert sunlight into electricity. While in a typical silicon photovoltaic device the semiconductor both absorbs light and transports charge carriers, the Grätzel cell separates these two functions as the dye absorbs photons and the titanium dioxide transports the charge-carrying electrons. Developed in response to the cost and manufacturing limitations of conventional photovoltaic technology, the Grätzel cell makes solar electricity more economically accessible.

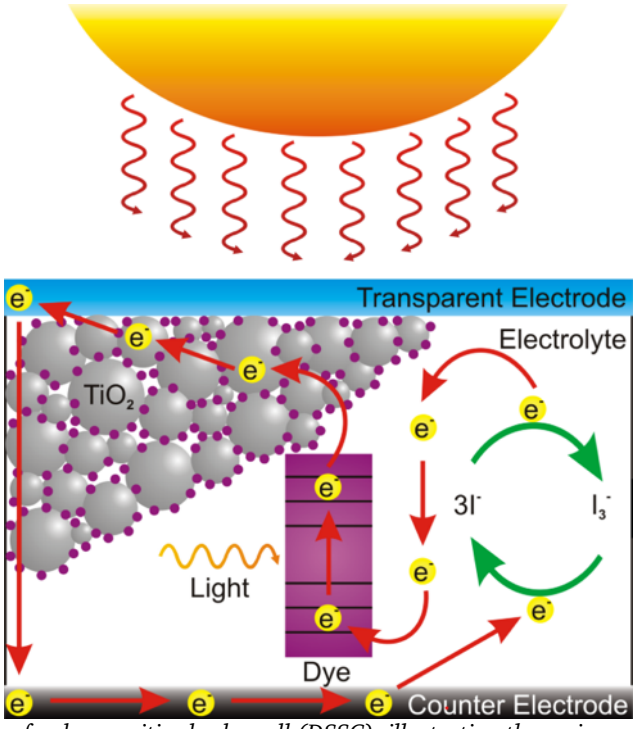


Figure 21. *Schematic diagram of a dye-sensitized solar cell (DSSC), illustrating the main components and electron-transfer pathway [21].*

The Grätzel cell can be divided into two main components: the photoanode and the counter electrode. The photoanode consists of conductive tin oxide glass coated with a porous nanocrystalline titanium dioxide film and light-absorbing dye. Since titanium dioxide has a wide band gap, it does not efficiently absorb much of the visible portion of sunlight. Instead, a dye absorbs the light and the photoexcited electrons are collected and transported through the titanium

dioxide [131]. The counter electrode consists of a conductive substrate coated with a catalyst, typically platinum because of its high catalytic activity. By catalyzing the reduction of iodide ions in the electrolyte, electrons donated to the oxidized dye promote regeneration so the cell can sustain numerous cycles without degradation.

Manufacturing Grätzel cells is challenging due to the high-temperature heat treatment required to achieve the desired porosity of the titanium dioxide particles and sinter them together to generate electrical connections and stabilize the film. Inexpensive and readily available plastic substrates are unable to withstand such high temperatures, creating a significant limitation to the production and accessibility of Grätzel cells. Another manufacturing challenge is sealing the cell to prevent electrolyte leakage and solvent evaporation which reduce long-term stability, while blocking harmful environmental factors like moisture and oxygen from entering the cell [132]. Several other factors such as titanium dioxide particle size, film thickness, dye absorption and sealing technique affect performance of the solar cell and must be considered before production.

Several variations of DSSCs have been developed to improve the efficiency, stability, and overall performance of the cell by altering the dye or electrolyte type. One of the most successful types uses ruthenium-based dyes for its broad absorption spectrum and photochemical stability; however, the high cost and limited availability of ruthenium have driven research toward organic dye alternatives [133]. Organic DSSCs use metal-free dyes with readily modifiable molecular structures to control light absorption and electronic properties, while reducing material costs and synthesis complexity. Other alternatives, such as co-sensitized DSSCs, combine two or more dyes with complementary absorption properties to broaden the range of dye absorbed. Beyond dye variance, solid-state DSSCs address liquid electrolyte limitations, solvent evaporation and electrolyte leakage, and improve long-term cell stability by replacing the liquid with a solid [134].

Modifying the sensitizer and electrolyte provide different strategies for improving the efficiency, stability, and practicality of Grätzel cells.

Grätzel cells demonstrate strong performance under diffuse and low-intensity light, producing significant power under indoor fluorescent and LED lighting. By generating energy in conditions where silicon-based solar cells generally perform less efficiently, DSSCs have the potential to power low-energy electronics that operate under indoor lighting. Moreover, studies demonstrate that Grätzel cells can be optimized for indoor use by selecting dye with absorption spectra matching indoor light wavelengths to further improve efficiency [135].

Conclusion

Solar energy conversion technology relies on a diverse set of materials and systems. Each has its own major trade-offs regarding conversion efficiency, material cost, durability, geographical suitability, and manufacturing complexity. Systems commonly used for solar conversion include photovoltaic cells, which convert light directly into electricity in semiconductor devices. Solar thermal collectors work by absorbing radiation to produce heat for water and other applications, through flat-plate, evacuated-tube, and concentrating designs offering different balances between cost and operating temperature. Concentrating photovoltaics work by focusing sunlight at a high ratio onto small high-efficiency cells, allowing for increased efficiencies at the cost of tracking requirements and higher material costs. Lastly, concentrating solar power towers work by using a large field of mirrors to heat a fluid at the central receiver to be used as thermal storage and generate energy at the cost of high investments and land use.

Common materials used in these systems include crystalline silicon, which is currently the most popular material, as monocrystalline cells have high efficiencies (22-24%) and great power densities. Polycrystalline cells, also made of crystalline silicon, trade some of the efficiency for

simpler processing and reduced cost. Amorphous silicon provides thin, flexible devices with good efficiency in low-light settings and a favorable temperature coefficient. However, it is limited by light degradation and lower efficiencies. Organic photovoltaics can be made with easier manufacturing processes and are flexible, but they struggle with how charges form, lifespan, and energy loss. CIGS thin film cells are able to achieve a competitive efficiency with low material requirements and have potential for use in flexible substrates. Although the high material costs of indium and gallium are drawbacks to its use, the material offers excellent performance and efficiency in solar energy applications. CdTe is a low-cost thin film technology with good commercial performance and has a straightforward manufacturing process. However, cadmium toxicity and tellurium supply restrict its use. Gallium-arsenide and III–V semiconductors have very high efficiencies and are widely used in multijunction and concentrated applications, but their high costs restrict them to niche markets. Grätzel cells are cheap to make and work well in low sunlight, but they have lower peak efficiencies and stability limitations compared to inorganic thin films.

Collectively, there is no single material or system that is universal. The selection of materials and systems depends on many factors, which include irradiance, temperature, land area, storage needs, and cost. However, major progress has been made since the development of these materials and systems to lower cost and raise efficiencies. Despite this, continued research into these systems and materials is still needed. Priorities in further research should include more stable and efficient light-absorbing materials, improved surface coating and contacts, cheaper and more durable parts, improved thermal storage, and manufacturing processes that reduce material use and have a lower environmental impact. Continued research into these areas is required to push efficiencies to the theoretical limit and improve their reliability over longer periods of time. Solar energy systems must be able to operate effectively under real-world conditions across diverse regions worldwide to increase their global use as an alternative to fossil fuels.

References

[1] Today's #TechTuesday invention is a solar engine from the 1907... | Hagley. (**2020**). Hagley.Org. https://www.hagley.org/research/news/hagley-vault/todays-techtuesday-invention-solar-engine-1907

[2] Van der Hoeven, D. (**2025**, April 8). Solar power plant's pioneer. Bio Based Press. https://www.biobasedpress.eu/2025/04/solar-power-plants-pioneer/

[3] rbradley. (**2025**, July 2). The First Solar Power Plant: 1916 - Master Resource. Master Resource. https://www.masterresource.org/solar-power-history/first-solar-grid-plant-1916/

[4] Solar Energy. (**2024**). Energy.Gov. https://www.energy.gov/topics/solar-energy

[5] Concentrating Solar-Thermal Power. (**2022**, September 21). Energy.Gov. https://www.energy.gov/cmei/systems/concentrating-solar-thermal-power

[6] Search for All Records | OSTI.GOV. (**2025**). Osti.Gov. https://www.osti.gov/search/sponsor-org:Solar%20Energy%20Technologies%20Offic

[7] IEA. (**2022**, July). Solar PV Global Supply Chains – Analysis. IEA. https://www.iea.org/reports/solar-pv-global-supply-chains

[8] Energy Technology Perspectives **2026** – Analysis - IEA. (2026, March 26). Energy Technology Perspectives 2026 – Analysis - IEA. IEA. https://www.iea.org/reports/energy-technology-perspectives-2026

[9] Solar Market Insight Report **2025** Year in Review – SEIA. (2025). SEIA. https://seia.org/research-resources/solar-market-insight-report-2025-year-in-review/

[10] Khamooshi, M., Salati, H., Egelioglu, F., Hooshyar Faghiri, A., Tarabishi, J., & Babadi, S. (**2014**). A Review of Solar Photovoltaic Concentrators. *International Journal of Photoenergy*, *2014*, 1–17. https://doi.org/10.1155/2014/958521

[11] Jing, L., Liu, H., Wang, Y., Xu, W., Zhang, H., & Lu, Z. (**2014**). Design and Optimization of Fresnel Lens for High Concentration Photovoltaic System. *International Journal of Photoenergy*, *2014*, 1–7. https://doi.org/10.1155/2014/539891

[12] Xie, W. T., Dai, Y. J., Wang, R. Z., & Sumathy, K. (**2011**). Concentrated solar energy applications using Fresnel lenses: A review. *Renewable and Sustainable Energy Reviews*, *15*(6), 2588–2606. https://doi.org/10.1016/j.rser.2011.03.031

[13] Mićić, O. I., Cheong, H. M., Fu, H., Zunger, A., Sprague, J. R., Mascarenhas, A., & Nozik, A. J. (**1997**). Size-Dependent Spectroscopy of InP Quantum Dots. *The Journal of Physical Chemistry B*, *101*(25), 4904–4912. https://doi.org/10.1021/jp9704731

[14] Garcia-Botella, A., Fernandez-Balbuena, A. A., Vázquez, D., & Bernabeu, E. (**2009**). Ideal 3D asymmetric concentrator. *Solar Energy*, *83*(1), 113–117. https://doi.org/10.1016/j.solener.2008.07.004

[15] Malato, S., Blanco, J., Vidal, A., & Richter, C. (**2001**). Photocatalysis with solar energy at a pilot-plant scale: an overview. *Applied Catalysis B: Environmental*, *37*(1), 1–15. https://doi.org/10.1016/S0926-3373(01)00315-0

[16] Clark, J. (**1982**). An analysis of the technical and economic performance of a parabolic trough concentrator for solar industrial process heat application. *International Journal of Heat and Mass Transfer*, *25*(9), 1427–1434. https://doi.org/10.1016/0017-9310(82)90136-3

[17] Suzuki, A., & Kobayashi, S. (**2000**). Yearly distributed insolation model and optimum design of a two-dimensional compound parabolic concentrator. *Solar Energy*, *54*(5), 327–331. https://doi.org/10.1016/0038-092X(95)00003-A

[18] Piszczor, M. F. J., & Macosko, R. P. (**2000**). A High-Efficiency Refractive Secondary Solar Concentrator for High Temperature Solar Thermal Applications. NASA Technical Reports Server. https://ntrs.nasa.gov/citations/20000081754

[19] Terao, A., Mulligan, W. P., Daroczi, S. G., Pujol, O. C., Verlinden, P. J., Swanson, R. M., Miñano, J. C., Benítez, P., & Álvarez, J. L. (**2000**). A mirror-less design for micro-concentrator modules. Conference Record of the Twenty-Eighth IEEE Photovoltaic Specialists Conference - 2000, 1416–1419. https://doi.org/10.1109/PVSC.2000.916158

[20] Maia, C. B., Rodrigues Neumann, L., de Andrade Oliveira, G., Marques Alves, Í., Walczak, M. M., & Paiva Brito, P. (**2023**). A comprehensive review of solar tower CSP systems using TES and molten salts. *International Journal of Ambient Energy*, *44*(1), 1733–1747. https://doi.org/10.1080/01430750.2023.2185814

[21] Boretti, A. (**2018**). Cost and production of solar thermal and solar photovoltaics power plants in the United States. *Renewable Energy Focus*, *26*, 93–99. https://doi.org/10.1016/j.ref.2018.07.002

[22] Aslam, Z., Gilani, S. I. U. H., Mohamad, T. I., Muhammad, M., & Alao, K. T. (**2025**). Technological frontiers and optimization in solar power towers: innovations in thermal energy storage, receivers, and heliostat systems. *Clean Technologies and Environmental Policy*, *27*(12), 8021–8049. https://doi.org/10.1007/s10098-025-03337-z

[23] Qaisrani, M. A., Wei, J., Fang, J., Jin, Y., Wan, Z., & Khalid, M. (**2019**). Heat losses and thermal stresses of an external cylindrical water/steam solar tower receiver. *Applied Thermal Engineering*, *163*, 114241. https://doi.org/10.1016/j.applthermaleng.2019.114241

[24] Wang, F., Shuai, Y., Yuan, Y., & Liu, B. (**2012**). Effects of material selection on the thermal stresses of tube receiver under concentrated solar irradiation. *Materials & Design*, *33*, 284–291. https://doi.org/10.1016/j.matdes.2011.07.048

[25] Commission, C. E. (n.d.). Genesis Solar Energy Project. California Energy Commission. *Retrieved August 29, 2026*, from https://www.energy.ca.gov/powerplant/solar-thermal/genesis-solar-energy-project

[26] SOLANA. (**2025**). Energy.Gov. https://www.energy.gov/edf/solana

[27] Mellit, A., & Kalogirou, S. (**2022**). 1—Solar radiation and photovoltaic systems: Modeling and simulation. In Handbook of Artificial Intelligence Techniques in Photovoltaic Systems (pp. 1–41). Academic Press. https://doi.org/10.1016/B978-0-12-820641-6.00001-6

[28] Shubbak, M. H. (**2019**). Advances in solar photovoltaics: Technology review and patent trends. *Renewable and Sustainable Energy Reviews*, *115*, 109383. https://doi.org/10.1016/j.rser.2019.109383

[29] Al-Ezzi, A. S., & Ansari, M. N. M. (**2022**). Photovoltaic Solar Cells: A Review. *Applied System Innovation*, *5*(4). https://doi.org/10.3390/asi5040067

[30] Al-Alwani, M. A. M., Mohamad, A. B., Ludin, N. A., Kadhum, A. A. H., & Sopian, K. (**2016**). Dye-sensitised solar cells: Development, structure, operation principles, electron kinetics, characterisation, synthesis materials and natural photosensitisers. *Renewable and Sustainable Energy Reviews*, *65*, 183–213. https://doi.org/10.1016/j.rser.2016.06.045

[31] Rehman, A. U., & Lee, S. H. (**2014**). Review of the Potential of the Ni/Cu Plating Technique for Crystalline Silicon Solar Cells. *Materials (Basel, Switzerland)*, *7*(2), 1318–1341. https://doi.org/10.3390/ma7021318

[32] Chen, C., Ran, C., Yao, Q., Wang, J., Guo, C., Gu, L., Han, H., Wang, X., Chao, L., Xia, Y., & Chen, Y. (**2023**). Screen-Printing Technology for Scale Manufacturing of Perovskite Solar Cells. *Advanced Science*, *10*(28), 2303992. https://doi.org/10.1002/advs.202303992

[33] Kadam, T. V., Pakhare, S. Y., & Godse, A. B. (**2025**). Performance analysis of solar thermal collectors: A comprehensive review. *Measurement: Energy*, *7*, Article 100059. https://doi.org/10.1016/j.meaene.2025.100059

[34] Wu, C., Zhao, Y., Li, W., Fan, J., Xu, H., Ling, Z., Yuan, D., & Zeng, X. (**2025**). Concentrated Solar Thermal Power Technology and Its Thermal Applications. *Energies*, *18*(8), 2120. https://doi.org/10.3390/en18082120

[35] Pathak, S. K., Tyagi, V. V., Chopra, K., B, K., Pandey, A. K., Goel, V., Saxena, A., & Ma, Z. (**2023**). Energy, exergy, economic and environmental analyses of solar air heating systems with and without thermal energy storage for sustainable development: A systematic review. *Journal of Energy Storage*, *59*, 106521. https://doi.org/10.1016/j.est.2022.106521

[36] Supankanok, R., Sriwong, S., Ponpo, P., Wu, W., Chandra-ambhorn, W., & Anantpinijwatna, A. (**2021**). Modification of a Solar Thermal Collector to Promote Heat Transfer inside an Evacuated Tube Solar Thermal Absorber. *Applied Sciences*, *11*(9), 4100. https://doi.org/10.3390/app11094100

[37] Saga, T. (**2010**). Advances in crystalline silicon solar cell technology for industrial mass production. *NPG Asia Materials*, *2*(3), 96–102. https://doi.org/10.1038/asiamat.2010.82

[38] Seo, D.-K., & Hoffmann, R. (**1999**). Direct and indirect band gap types in one-dimensional conjugated or stacked organic materials. *Theoretical Chemistry Accounts: Theory, Computation, and Modeling (Theoretica Chimica Acta)*, *102*(1–6), 23–32. https://doi.org/10.1007/s002140050469

[39] Battaglia, C., Cuevas, A., & De Wolf, S. (**2016**). High-efficiency crystalline silicon solar cells: Status and perspectives. *Energy & Environmental Science*, *9*(5), 1552–1576. https://doi.org/10.1039/c5ee03380b

[40] Radiative recombination. (n.d.). In ScienceDirect Topics. *Retrieved August 18, 2026*, from https://www.sciencedirect.com/topics/engineering/radiative-recombination

[41] Auger recombination. (n.d.). In ScienceDirect Topics. *Retrieved August 18, 2026*, from https://www.sciencedirect.com/topics/engineering/auger-recombination

[42] Zanatta, A. R. (**2022**). The Shockley–Queisser limit and the conversion efficiency of silicon-based solar cells. *Results in Optics*, *9*, 100320. https://doi.org/10.1016/j.rio.2022.100320

[43] Jiang, L., Cui, S., Sun, P., Wang, Y., & Yang, C. (**2020**). Comparison of monocrystalline and polycrystalline solar modules. In 2020 IEEE 5th Information Technology and Mechatronics Engineering Conference (ITOEC) (pp. 341–344). IEEE. https://doi.org/10.1109/ITOEC49072.2020.9141722

[44] Ray, M., Kabir, M. F., Raihan, M., Bhuiyan, A. B. M. N., Akand, T., & Mohammad, N. (**2023**). Performance evaluation of monocrystalline and polycrystalline-based solar cell. *International Journal of Energy and Environmental Engineering*, *14*(4), 949–960. https://doi.org/10.1007/s40095-023-00558-0

[45] Czochralski process. (**2019**). In ScienceDirect Topics. https://www.sciencedirect.com/topics/chemistry/czochralski-process

[46] Which Is More Efficient, Monocrystalline Silicon Or Polycrystalline Silicon - BLOG - Tongwei Co., Ltd.,. (**2024**). In Tongwei.cn. https://en.tongwei.cn/blog/201.html

[47] Adolf, K., & Afam Uzorka. (**2025**). Effects of substrates on the efficiency of a monocrystalline solar panel. *Scientific Reports*, *15*(1). https://doi.org/10.1038/s41598-025-90523-0

[48] Manalu, Y. A., & Anisah, S. (**2025**). Comparative analysis of polycrystalline and monocrystalline solar panels in PV systems. In International Conference of Digital Sciences and Engineering Technology (pp. 337–346). https://proceeding.pancabudi.ac.id/index.php/ICDSET/article/view/359

[49] Cost Breakdown Monocrystalline vs. Polycrystalline Solar Panels - BLOG - Tongwei Co., Ltd.,. (**2023**). In Tongwei.cn. https://en.tongwei.cn/blog/26.html

[50] NASA. (n.d.). Solar irradiance science. Retrieved October 2026, from https://earth.gsfc.nasa.gov/climate/projects/solar-irradiance/science

[51] Mirzaei, M., & Mohiabadi, M. Z. (**2017**). A comparative analysis of long-term field test of monocrystalline and polycrystalline PV power generation in semi-arid climate conditions. *Energy for Sustainable Development*, *38*, 93–101. https://doi.org/10.1016/j.esd.2017.01.002

[52] Kumari, N., Singh, S. K., Kumar, S., & Jadoun, V. K. (**2024**). Performance analysis of partially shaded high-efficiency mono PERC/mono crystalline PV module under indoor and environmental conditions. *Scientific Reports*, *14*(1). https://doi.org/10.1038/s41598-024-72502-z

[53] Benghanem, M., Haddad, S., Alzahrani, A., Mellit, A., AlMohamadi, H., Khushaim, M., & Aida, M. S. (**2023**). Evaluation of the performance of polycrystalline and monocrystalline PV technologies in a hot and arid region: An experimental analysis. *Sustainability*, *15*(20), Article 14831. https://doi.org/10.3390/su152014831

[54] Kazem, H. A., Chaichan, M. T., & Al-Waeli, A. H. A. (**2022**). A comparison of dust impacts on polycrystalline and monocrystalline solar photovoltaic performance: an outdoor experimental study. Environmental Science and Pollution Research. https://doi.org/10.1007/s11356-022-21958-5

[55] Ayadi, O., Shadid, R., Bani-Abdullah, A., Alrbai, M., Abu-Mualla, M., & Balah, N. (**2022**). Experimental comparison between Monocrystalline, Polycrystalline, and Thin-film solar systems under sunny climatic conditions. *Energy Reports*, *8*(9), 218–230. https://doi.org/10.1016/j.egyr.2022.06.121

[56] Kabir, M. I., Ibrahim, Z., Sopian, K., & Amin, N. (**2010**). Effect of structural variations in amorphous silicon based single and multi-junction solar cells from numerical analysis. *Solar Energy Materials and Solar Cells*, *94*(9), 1542–1545. https://doi.org/10.1016/j.solmat.2009.12.031

[57] Amorphous silicon. (n.d.). In ScienceDirect Topics. *Retrieved August 19, 2026*, from https://www.sciencedirect.com/topics/earth-and-planetary-sciences/amorphous-silicon

[58] Sreejith, S., Ajayan, J., Kollem, S., & Sivasankari, B. (**2022**). A Comprehensive Review on Thin Film Amorphous Silicon Solar Cells. Silicon. https://doi.org/10.1007/s12633-021-01644-w

[59] Rech, B., & Wagner, H. (**1999**). Potential of amorphous silicon for solar cells. *Applied Physics A: Materials Science & Processing*, *69*(2), 155–167. https://doi.org/10.1007/s003390050986

[60] Qarony, W., Hossain, M. I., Hossain, M. K., Uddin, M. J., Haque, A., Saad, A. R., & Tsang, Y. H. (**2017**). Efficient amorphous silicon solar cells: characterization, optimization, and optical loss analysis. *Results in Physics*, *7*, 4287–4293. https://doi.org/10.1016/j.rinp.2017.09.030

[61] T Markvart, & Castañer, L. (**2003**). Practical handbook of photovoltaics : fundamentals and applications. Elsevier. https://www.sciencedirect.com/science/chapter/edited-volume/abs/pii/B9781856173902500131

[62] Best Research-Cell Efficiency Chart | Photovoltaic Research | NLR. (**2025**). In Nlr.gov. https://www.nlr.gov/pv/cell-efficiency

[63] Yang, J., Yan, B., & Guha, S. (**2005**). Amorphous and nanocrystalline silicon-based multi-junction solar cells. *Thin Solid Films*, *487*(1–2), 162–169. https://doi.org/10.1016/j.tsf.2005.01.058

[64] Smith, D. D., Cousins, P., Westerberg, S., Jesus-Tabajonda, R. De, Aniero, G., & Shen, Y.-C. (**2014**). Toward the Practical Limits of Silicon Solar Cells. *IEEE Journal of Photovoltaics*, *4*(6), 1465–1469. https://doi.org/10.1109/jphotov.2014.2350695

[65] Staebler, D. L., Crandall, R. S., & Williams, R. (**1981**). Stability of n-i-p amorphous silicon solar cells. *Applied Physics Letters*, *39*(9), 733–735. https://pubs.aip.org/aip/apl/article-abstract/39/9/733/525101/Stability-of-n-i-p-amorphous-silicon-solar-cells

[66] Rüther, R., & Livingstone, J. (**1995**). Seasonal variations in amorphous silicon solar module outputs and thin film characteristics. *Solar Energy Materials and Solar Cells*, *36*(1), 29–43. https://doi.org/10.1016/0927-0248(94)00165-o

[67] Lund, C. P., Luczak, K., Pryor, T., Cornish, J. C. L., Jennings, P. J., Knipe, P., & Ahjum, F. (**2001**). Field and laboratory studies of the stability of amorphous silicon solar cells and modules. *Renewable Energy*, *22*(1–3), 287–294. https://doi.org/10.1016/s0960-1481(00)00045-8

[68] King, D. L., Kratochvil, J. A., & Boyson, W. E. (**2000**). Stabilization and performance characteristics of commercial amorphous-silicon PV modules. Conference Record of the Twenty-Eighth IEEE Photovoltaic Specialists Conference - 2000 (Cat. No.00CH37036), 1446–1449. https://doi.org/10.1109/pvsc.2000.916165

[69] Maluta, E., & Sankaran, V. (**2011**). Outdoor testing of amorphous and crystalline silicon solar panels at Thohoyandou. *Journal of Energy in Southern Africa*, *22*(3), 16–22. https://www.scielo.org.za/scielo.php?pid=S1021-447X2011000300003&script=sci_arttext

[70] Galloni, R. (**1996**). Amorphous silicon solar cells. *Renewable Energy*, *8*(1–4), 400–404. https://doi.org/10.1016/0960-1481(96)88886-0

[71] Rech, B., & Wagner, H. (**1999**). Potential of amorphous silicon for solar cells. *Applied Physics A: Materials Science & Processing*, *69*(2), 155–167. https://doi.org/10.1007/s003390050986

[72] Shah, A., Meier, J., Buechel, A., Kroll, U., Steinhauser, J., Meillaud, F., Schade, H., & Dominé, D. (**2006**). Towards very low-cost mass production of thin-film silicon photovoltaic (PV) solar modules on glass. *Thin Solid Films*, *502*(1–2), 292–299. https://doi.org/10.1016/j.tsf.2005.07.299

[73] Shah, A. V., Platz, R., & Keppner, H. (**2000**). Thin-film silicon solar cells: A review and selected trends. *Solar Energy Materials and Solar Cells*, *38*(1–4), 501–520. https://doi.org/10.1016/0927-0248(94)00241-X

[74] Street, R. (**1999**). Technology and applications of amorphous silicon. Springer Science & Business Media. https://books.google.com/books?id=tZFyXvnoHUEC

[75] Wu, J., Gao, M., Chai, Y., Liu, P., Zhang, B., Liu, J., & Ye, L. (**2021**). Towards a bright future: The versatile applications of organic solar cells. *Materials Reports: Energy*, *1*(4), 100062. https://doi.org/10.1016/j.matre.2021.100062

[76] Organic solar cells. (**2013**). In ScienceDirect Topics. https://www.sciencedirect.com/topics/materials-science/organic-solar-cells

[77] Chen, H., Huang, Y., Zhang, R., Mou, H., Ding, J., Zhou, J., Wang, Z., Li, H., Chen, W., Zhu, J., Cheng, Q., Gu, H., Wu, X., Zhang, T., Wang, Y., Zhu, H., Xie, Z., Gao, F., Li, Y., & Li, Y. (**2025**). Organic solar cells with 20.82% efficiency and high tolerance of active layer thickness through crystallization sequence manipulation. *Nature Materials*, *24*, 444–453. https://doi.org/10.1038/s41563-024-02062-0

[78] Hains, A. W., Liang, Z., Woodhouse, M. A., & Gregg, B. A. (**2010**). Molecular Semiconductors in Organic Photovoltaic Cells. *Chemical Reviews*, *110*(11), 6689–6735. https://doi.org/10.1021/cr9002984

[79] BERNÈDE, J. C. (**2008**). ORGANIC PHOTOVOLTAIC CELLS: HISTORY, PRINCIPLE AND TECHNIQUES. *Journal of the Chilean Chemical Society*, *53*(3). https://doi.org/10.4067/s0717-97072008000300001

[80] Cui, Y., Yao, H., Zhang, J., Xian, K., Zhang, T., Hong, L., Wang, Y., Xu, Y., Ma, K., An, C., He, C., Wei, Z., Gao, F., & Hou, J. (**2020**). Single-junction organic photovoltaic cells with approaching 18% efficiency. *Advanced Materials*, *32*, Article 1908205. https://doi.org/10.1002/adma.201908205

[81] Zhang, G., Lin, F., Qi, F., Heumueller, T., Distler, A., Hans-Joachim Egelhaaf, Li, N., Chow, P. I., Brabec, C. J., Alex K.-Y. Jen, & Yip, H.-L. (**2022**). Renewed Prospects for Organic Photovoltaics. *Chemical Reviews*, *122*(18), 14180–14274. https://doi.org/10.1021/acs.chemrev.1c00955

[82] Solak, E. K., & Irmak, E. (**2023**). Advances in organic photovoltaic cells: a comprehensive review of materials, technologies, and performance. *RSC Advances*, *13*(18), 12244–12269. https://doi.org/10.1039/d3ra01454a

[83] Forrest, S. R. (**2005**). The Limits to Organic Photovoltaic Cell Efficiency. *MRS Bulletin*, *30*(1), 28–32. https://doi.org/10.1557/mrs2005.5

[84] Sampaio, P. G. V., & González, M. O. A. (**2022**). A review on organic photovoltaic cell. *International Journal of Energy Research*, *46*(13), 17813–17828. https://doi.org/10.1002/er.8456

[85] Seki, K., Furube, A., & Yoshida, Y. (**2013**). Detailed balance limit of power conversion efficiency for organic photovoltaics. *Applied Physics Letters*, *103*(25). https://pubs.aip.org/aip/apl/article-abstract/103/25/253904/26119/Detailed-balance-limit-of-power-conversion?redirectedFrom=fulltext

[86] Luo, W., Khaing, A. M., Rodriguez-Gallegos, C. D., Leow, S. W., Reindl, T., & Pravettoni, M. (**2024**). Long-term outdoor study of an organic photovoltaic module for building

integration. *Progress in Photovoltaics: Research and Applications*, *32*(7), 481–491. https://doi.org/10.1002/pip.3791

[87] Liu, S., Zhang, D., Egelhaaf, H.-J., Wang, G., Li, X., Heumüller, T., Brabec, C. J., & Li, N. (**2024**). Analyzing the outdoor degradation behavior of organic solar modules in North China. *Journal of Materials Chemistry A*, *12*(24), 14688–14697. https://doi.org/10.1039/d4ta00493k

[88] Xu, H., Han, J., Babics, M., Huerta Hernandez, L., Rosas Villalva, D., Sanviti, M., Bertrandie, J., Zhang, Y., Liu, Y., Chen, H., Zhao, L., Troughton, J., Martin, J., Laquai, F., De Wolf, S., & Baran, D. (**2025**). Elucidating the photodegradation pathways of polymer donors for organic solar cells with seven months of outdoor operational stability. *Nature Photonics*, *19*(4), 415–425. https://doi.org/10.1038/s41566-025-01644-x

[89] López, J. J. P., Rivera Botia, K. G., Ballestas, K., Velilla, E., Montoya, J. F., Jaramillo, F., & Ramirez, D. (**2026**). The long road to outdoor stability: real-world challenges for controlling perovskite materials for solar cells. *Chemical Society Reviews*. https://doi.org/10.1039/d5cs01085c

[90] Burlingame, Q., Huang, X., Liu, X., Jeong, C., Coburn, C., & Forrest, S. R. (**2019**). Intrinsically stable organic solar cells under high-intensity illumination. *Nature*, *573*(7774), 394–397. https://doi.org/10.1038/s41586-019-1544-1

[91] Mattiasson Bjuggren, J., Marsh, T., Al-Ahmad, A., Sivunova, K., Bonham, M., Clifton, S., Nicolaidis, N., Belcher, W., & Dastoor, P. (**2025**). Determining the Cost of Organic Photovoltaic Material and Its Impact on the Levelized Cost of Electricity. *Journal of Electronic Materials*. https://doi.org/10.1007/s11664-025-11826-6

[92] Chen, X., Hu, L., Li, C., Wang, C., Zhang, Z., Shi, J., Cui, H., & Chen, C. (**2026**). Perovskite/copper indium gallium selenide tandem solar cells. *ACS Omega*, *11*(15), 22479–22495. https://doi.org/10.1021/acsomega.6c01001

[93] Department of Materials Science and Metallurgy - University of Cambridge. (n.d.). *Direct and Indirect Band Gap Semiconductors*. University of Cambridge. https://www.doitpoms.ac.uk/tlplib/semiconductors/direct.php

[94] Teknetzi, I., Nguyen, H. C., Holgersson, S., & Ebin, B. (**2026**). Selective recovery of the CIGS and Mo layers from thin film solar cells. *Solar Energy Materials and Solar Cells*, *300*, Article 114237. https://doi.org/10.1016/j.solmat.2026.114237

[95] Zhou, J., & Li, C. (**2021**). Research on copper indium gallium selenide (CIGS) thin-film solar cells. *E3S Web of Conferences*, *267*, Article 02031. https://doi.org/10.1051/e3sconf/202126702031

[96] Adhikari, A., Acosta-Najarro, D. R., Fragoso-Medina, A. J., Reyes-Vallejo, O., Cano, F. J., Olvera Amador, M. de la L., & Subramaniam, V. (**2024**). Review on the developments in copper indium gallium diselenide (CIGSe)-based thin film photovoltaic devices. *Journal of Materials Science: Materials in Electronics*, *35*, Article 1016. https://doi.org/10.1007/s10854-024-12658-6

[97] Heinemann, M. D., Efimova, V., Klenk, R., Hoepfner, B., Wollgarten, M., Unold, T., Schock, H.-W., & Kaufmann, C. A. (**2015**). Cu(In,Ga)Se2 superstrate solar cells: Prospects and limitations. *Progress in Photovoltaics: Research and Applications*, *23*, 1228–1237. https://doi.org/10.1002/pip.2536

[98] Heinemann, M. D. (**2016**). CIGSe superstrate solar cells: Growth and characterization of CIGSe thin films on transparent conductive oxides [Doctoral dissertation, Technische Universität Berlin]. DepositOnce. https://doi.org/10.14279/depositonce-5097

[99] Li, W., Yan, X., Xu, W.-L., Long, J., Aberle, A. G., & Venkataraj, S. (**2017**). Efficiency improvement of CIGS solar cells by a modified rear contact. *Solar Energy*, *157*, 486–495. https://doi.org/10.1016/j.solener.2017.08.054

[100] Prasad, R., Das, A. K., & Singh, U. P. (**2021**). Impact of buffer layers on the performance of graded CIGS solar cells: A numerical approach. *Applied Physics A*, *127*, Article 816. https://doi.org/10.1007/s00339-021-04954-3

[101] Rahman, M. F., Hasan, M. K., Chowdhury, M., Islam, M. R., Rahman, M. H., Rahman, M. A., Al Ahmed, S. R., Ismail, A. B. M., Amami, M., Hossain, M. K., & Al-Hazmi, G. A. A. M. (**2023**). A qualitative design and optimization of CIGS-based solar cells with Sn2S3 back surface field: A plan for achieving 21.83% efficiency. *Heliyon*, *9*(12), Article e22866. https://doi.org/10.1016/j.heliyon.2023.e22866

[102] Rafati Rahimzadeh, M., Rafati Rahimzadeh, M., Kazemi, S., & Moghadamnia, A.-A. (**2017**). *Cadmium toxicity and treatment: An update*. Caspian journal of internal medicine. https://pmc.ncbi.nlm.nih.gov/articles/PMC5596182/

[103] Ravilla, A., Gullickson, E., Tomes, A., & Celik, I. (**2024**). Economic and environmental sustainability of copper indium gallium selenide (CIGS) solar panels recycling. *Science of The Total Environment*, *951*, Article 175670. https://doi.org/10.1016/j.scitotenv.2024.175670

[104] Tabbakh, T. A., Aljohany, R. M., Alhazmi, H., & Alsulami, R. M. (**2020**). Elastic, optical, transport, and structural properties of GaAs. In M. M. Rahman, A. M. A. Asiri, T. A. Tabbakh, A. Khan, & Inamuddin (Eds.), *Post-transition metals*. IntechOpen. https://doi.org/10.5772/intechopen.94566

[105] Indium. Daily Metal Prices. (n.d.). https://www.dailymetalprice.com/indium.html

[106] *What are CIGS thin-film solar panels? when to use them?*. Solar Magazine. (**2022**, March 6). https://solarmagazine.com/solar-panels/cigs-thin-film-solar-panels/

[107] Han, C. (**2020**). Analysis of moisture-induced degradation of thin-film photovoltaic module. *Solar Energy Materials and Solar Cells*, *210*, Article 110488. https://doi.org/10.1016/j.solmat.2020.110488

[108] Lin, L., & Ravindra, N. M. (**2020**). Temperature dependence of CIGS and perovskite solar cell performance: An overview. *SN Applied Sciences*, *2*, Article 1361. https://doi.org/10.1007/s42452-020-3169-2

[109] Gözükızıl, M. F. (**2025**). Efficiency analysis of organic, perovskite, and CIGS solar cells: Determination of photovoltaic parameters under different weather conditions. *Optical and Quantum Electronics*, *57*, Article 212. https://doi.org/10.1007/s11082-025-08140-0

[110] Chauhan, S., Sharma, A. K., & Singha, N. S. (**2025**). On the performance and thermal stability of solar cell based on CIGS-Sb2S3 combination with >35% power conversion efficiency. *Solid State Communications*, *395*, Article 115736. https://doi.org/10.1016/j.ssc.2024.115736

[111] Carcia, P. F., McLean, R. S., & Hegedus, S. (**2010**). Encapsulation of Cu(InGa)Se2 solar cell with Al2O3 thin-film moisture barrier grown by atomic layer deposition. *Solar Energy Materials and Solar Cells*, *94*(12), 2375–2378. https://doi.org/10.1016/j.solmat.2010.08.021

[112] Manimaran, U., & Dangate, M. S. (**2025**). A review on conducting materials in CdTe photovoltaic cells. *ACS Omega*, *10*(23), 23858–23872. https://doi.org/10.1021/acsomega.5c01030

[113] Cadmium telluride solar cell. (n.d.). In ScienceDirect Topics. https://www.sciencedirect.com/topics/engineering/cadmium-telluride-solar-cell

[114] Ahmad, N. I., Kar, Y. B., Doroody, C., Kiong, T. S., Rahman, K. S., Harif, M. N., & Amin, N. (**2023**). A comprehensive review of flexible cadmium telluride solar cells with back surface field layer. *Heliyon*, *9*(11), Article e21622. https://doi.org/10.1016/j.heliyon.2023.e21622

[115] Zheng, X., Kuciauskas, D., Moseley, J., Colegrove, E., Albin, D. S., Moutinho, H., Duenow, J. N., Ablekim, T., Harvey, S. P., Ferguson, A., & Metzger, W. K. (**2019**). Recombination and bandgap engineering in CdSeTe/CdTe solar cells. *APL Materials*, *7*(7), Article 071112. https://doi.org/10.1063/1.5098459

[116] Superstrate configuration. (n.d.). In ScienceDirect Topics. https://www.sciencedirect.com/topics/engineering/superstrate-configuration

[117] Manimaran, U., & Dangate, M. S. (**2025**). A review on conducting materials in CdTe photovoltaic cells. *ACS Omega*, *10*(23), 23858–23872. https://doi.org/10.1021/acsomega.5c01030

[118] Tai, Y., Zhang, X., Li, J., Zheng, Y., Liu, G., Zhang, J., Zeng, G., Yakubov, K., & Chebotareva, A. (**2025**, January). Research on ultra-thin cadmium telluride heterojunction thin film solar cells. Renewable and Sustainable Energy Reviews. https://doi.org/10.1016/j.rser.2024.114996

[119] Prasad, R., Das, A. K., & Singh, U. P. (**2021**). Impact of buffer layers on the performance of graded CIGS solar cells: A numerical approach. *Applied Physics A*, *127*, Article 816. https://doi.org/10.1007/s00339-021-04954-3

[120] Bätzner, D. L., Wendt, R., Romeo, A., Zogg, H., & Tiwari, A. N. (**2000**, February 21). A study of the back contacts on CdTe/CdS solar cells. Thin Solid Films. https://doi.org/10.1016/S0040-6090(99)00842-1

[121] Sartor, B. E., Zhang, T., Muzzillo, C. P., Lee, C., Muzzio, R., Gogotsi, Y., Reese, M. O., & Taylor, A. D. (**2024**). Hierarchical transparent back contacts for bifacial CdTe PV. *ACS Energy Letters*, *9*(4), 1617–1623. https://doi.org/10.1021/acsenergylett.4c00156

[122] Urbaniak, A., Lichocki, E., Czudek, A., & Würz, R. (**2025**, August 1). The impact of grain boundary defects on the current-voltage characteristics of Cu(In,Ga)Se2-based solar cells. Thin Solid Films. https://doi.org/10.1016/j.tsf.2025.140702

[123] Deep impurity level. (n.d.). In ScienceDirect Topics. https://www.sciencedirect.com/topics/chemistry/deep-impurity-level

[124] Tong, C.-J., & McKenna, K. P. (**2019**). Passivating grain boundaries in polycrystalline CdTe. *The Journal of Physical Chemistry C*, *123*(39), 23882–23889. https://doi.org/10.1021/acs.jpcc.9b08373

[125] First Solar. (n.d.). First Solar: A leading global provider of comprehensive PV solar solutions. https://www.firstsolar.com/

[126] Mehdi, M., Ammari, N., Alami Merrouni, A., El Gallassi, H., Dahmani, M., & Ghennioui, A. (**2023**, March). An experimental comparative analysis of different PV technologies performance including the influence of hot-arid climatic parameters: Toward a realistic yield assessment for desert locations. Renewable Energy. https://doi.org/10.1016/j.renene.2023.01.082

[127] Solaria Solar and Roofing Resize. (**2026**, April 6). Cadmium telluride solar panels vs. silicon. https://solariasolarandroofing.com/cadmium-telluride-solar-panels-vs-silicon-which-is-more-efficient-in-2025/

[128] González-Morales, M. A., Cruz-Bueno, J. J., Villa-Martínez, G., Ramírez-López, M., Flores-Ramírez, D., Rodríguez-Fragoso, P., Herrera-Pérez, J. L., Casallas-Moreno, Y. L., & Mendoza-Álvarez, J. G. (**2022**). Importance of liquid phase epitaxy on achieving near-lattice-matched growth of $In_{0.145}Ga_{0.855}As_{0.132}Sb_{0.868}$ layers on GaSb(100) substrates. *Superficies y Vacío, 35*, 220601. https://doi.org/10.47566/2022_syv35_1-220601

[129] Squintinjones. (**2025**, October 16). *Band gap for gallium arsenide (GaAs)* [Image]. Wikimedia Commons. https://commons.wikimedia.org/wiki/File:Band_Gap_for_Gallium_Arsenide_(GaAs).png

[130] Kiessling, F.-M., Rudolph, P., Neubert, M., Juda, U., Naumann, M., & Ulrici, W. (**2004**). Growth of GaAs crystals from Ga-rich melts by the VCz method without liquid encapsulation. *Journal of Crystal Growth, 269*(2–4), 218–228. https://doi.org/10.1016/j.jcrysgro.2004.04.124

[131] O'Regan, B., & Grätzel, M. (**1991**). A low-cost, high-efficiency solar cell based on dye-sensitized colloidal TiO_2 films. *Nature, 353*(6346), 737–740. https://doi.org/10.1038/353737a0

[132] Kokkonen, M., Talebi, P., Zhou, J., Asgari, S., Soomro, S. A., Elsehrawy, F., Halme, J., Ahmad, S., Hagfeldt, A., & Hashmi, S. G. (**2021**). Advanced Research trends in dye-

sensitized solar cells. *Journal of Materials Chemistry A*, *9*(17), 10527–10545. https://doi.org/10.1039/d1ta00690h

[133] Vougioukalakis, G. C., Philippopoulos, A. I., Stergiopoulos, T., & Falaras, P. (**2011**). Contributions to the development of ruthenium-based sensitizers for dye-sensitized solar cells. *Coordination Chemistry Reviews, 255*(21–22), 2602–2621. https://doi.org/10.1016/j.ccr.2010.11.006

[134] Benesperi, I., Michaels, H., & Freitag, M. (**2018**). The researcher's guide to solid-state dye-sensitized solar cells. *Journal of Materials Chemistry C, 6*(44), 11903–11942. https://doi.org/10.1039/C8TC03542C

[135] Devadiga, D., Selvakumar, M., Shetty, P., & Santosh, M. S. (**2021**). Dye-sensitized solar cell for indoor applications: A mini-review. *Journal of Electronic Materials, 50*(6), 3187–3206. https://doi.org/10.1007/s11664-021-08854-3

[136] Zhu, L., Zhang, M., Zhou, Z., Zhong, W., Hao, T., Xu, S., Zeng, R., Zhuang, J., Xue, X., Jing, H., Zhang, Y., & Liu, F. (**2024**). Progress of organic photovoltaics towards 20% efficiency. *Nature Reviews Electrical Engineering*. https://doi.org/10.1038/s44287-024-00080-3

[137] *Indium*. American Chemical Society. (n.d.). https://www.acs.org/green-chemistry-sustainability/research-innovation/endangered-elements/indium.html

[138] Solar Energy Research Areas. (**2017**, April 20). Energy.Gov. https://www.energy.gov/cmei/systems/solar-energy-research-areas